TESTING OF AIRCRAFT COMPOSITE SPOILER HINGES

MUHAMMAD ZUHRI ZIKIRILAH BIN MOHD KURMAIN

UNIVERSITI TEKNIKAL MALAYSIA MELAKA

TESTING OF AIRCRAFT COMPOSITE SPOILER HINGES

MUHAMMAD ZUHRI ZIKIRILAH BIN MOHD KURMAIN

This report is submitted
in fulfillment of the requirement for the degree of
Bachelor of Mechanical Engineering (Structure and Material)

Faculty of Mechanical Engineering

UNIVERSITI TEKNIKAL MALAYSIA MELAKA

2017

DECLARATION

I declare that this project report entitled “Testing of Aircraft Composite Spoiler Hinges ” is the result of my own work except as cited in the references.

Signature : ....

Name : ....

Date : ....

APPROVAL

I hereby declare that I have read this project report and in my opinion this report is sufficient in terms of scope and quality for the award of the degree of Bachelor of Mechanical Engineering (Structure & Materials).

Signature :. ....

Name of Supervisor : ....

Date : ....

DEDICATION

Special dedicated,

To my beloved family,

Thanks for your morale support and understanding.

To my lovely friends,

Thanks you for all help

May God bless all of your kindness

ABSTRACT

Nowadays, Composite material is a major interest in many industries especially in aviation manufacturing. The transformation of composite over metallic material is due to high strength but light weight which indirectly contributes to save fuel consumption of aircraft. Almost entire structure of aircraft has changed to various types of composite material but only current hinge bracket for A320 aircraft are still made from metallic materials. The structure of hinges bracket are only analyzed by using Finite Element Method (FEM) analysis due to limitation of time and cost. However, this thesis is concerned with the experimental testing method in laboratory to analyze the structure of aircraft composite spoiler hinges. The several custom jigs for tester machine are developed to adapt the real condition in laboratory. The compression testing approach was used to analyze the structure of composite spoiler hinges after the real condition of aircraft testing cannot be replicated due to slipping of custom jig. The analysis of composite hinges by experimental testing is involved the comparing and validating with simulation and theoretical result in term of deflection and failure location. The failure location occurred on composite spoiler hinges by experimental almost similar to the prediction of simulation finite element method. But, the deflection of composite hinge for experiment testing was greater than theoretical and simulation finite element method by 61 and 63 percent, respectively due to imperfection and defect of the composite spoiler hinges prototypes. It is hope that this research will be able to help other researcher on further investigation of laminated composite in aircraft structure.

ABSTRAK

Pada masa kini, komposit merupakan bahan yang menjadi kepentigan utama dipelbagai sektor industri terutamanya didalam pembuatan struktur pesawat. Transformasi bahan komposit daripada bahan logam disebabkan oleh kekuatan yang tinggi malah lebih ringan secara tidak langsung menyumbang kepada penjimatan bahan bakar pesawat. Hampir keseluruhan struktur pesawat telah berubah kepada pelbagai jenis bahan komposit tetapi hanya pendakap engsel bagi pesawat A320 masih dibuat daripada bahan logam. Penganalisaan strutuktur bagi pendakap engsel hanya dibuat melalui Kaedah Unsur Terhingga (FEM) kerana oleh batasan masa dan kos. Walaubagaimanapun, karya ini adalah berkenaan dengan kaedah ujian eksperimen dalam makmal untuk menganalisis struktur pesawat komposit engsel spoiler. Beberapa jig khas untuk mesin penguji telah dibangunkan supaya dapat menyesuaikan keadaan sebenar dengan keadaan didalam makmal. Pendekatan ujian mampatan telah digunakan untuk menganalisa struktur komposit engsel spoiler dimana selepas ujian sebenar tidak dapat dilakukan disebabakan oleh jig ujian tergelincir. Analisis komposit engsel ini melibatkan perbandingan dan pengesahan dengan simulasi dan hasil teori didalam bentuk perubahan pesongan dan lokasi kegagalan. Lokasi kegagalan berlaku oleh eksperimentasi hampir sama dengan ramalan yang dibuat secara simulasi. Akan tetapi, perubahan pesongan engsel bagi ujian eksperimentasi adalah lebih besar daripada hasil teori dan simulasi kaedah unsur terhingga sebanyak 61 dan 63 masing-masing. Hal ini disebabkan oleh ketidaksempurnaan dan kecacatan pada komposit spoiler engsel. Ianya berharap agar kajian ini dapat memberi sedikit pentunjuk bagi siasatan lanjut dalam komposit berlapis bagi struktur pesawat.

ACKNOWLEDGEMENTS

In The Name of GOD, Most Gracious, Most Merciful

I would like to thank Centre for Research and Innovation Management (CRIM) and Faculty of Mechanical Engineering (FKM) Universiti Teknikal Malaysia Melaka for funding this research and having interest in this area of engineering. I hope that the contents of this thesis can benefit them in the further design and development of their laminated composite structures.

I would like to thank my supervisors, Associate Professor Ahmad Rivai for his suggestions and guidance. I would also like to thank my parents, family members, roommates and other friends who were involved directly or indirectly in completion of my thesis. Although I cannot mention them all by name, I am grateful to all of them and wish them all the best. Thank you for your morale support throughout my graduate studies.

Last but not least, I would like to thank God for answering my prayers in my darkest times. The completion of this thesis would not been possible without His's will. I humbly thank you for guiding and instilling faith in me.

TABLE OF CONTENTS

LIST OF TABLE

LIST OF FIGURES

LIST OF APPENDICES

LIST OF ABBREVIATIONS

2D	-	Two dimensional
3D	-	Three dimensional
ASME	-	American Society of Mechanical Engineers
ASTM	-	American Society for Testing and Materials
CAD	-	Computer Aided Design
cm	-	centimeter
cm^3	-	centimeter cubic
CTRM	-	Composite Technology Research Malaysia
Etc.	-	Et cetera
FEA	-	Finite Element Analysis
FEM	-	Finite Element Method
FRP	-	Fiber Reinforced Polymer
FPF	-	First ply failure
g	-	Gram
g/cm^3	-	Gram per centimeter cube
mm	-	millimeters
mm2	-	millimeters square
mm3	-	millimeters cube
MPa	-	MegaPascal

N	-	Newton
Nm	-	Newton meter
NASA	-	The National Aeronautics and Space Administration
UD	-	Unidirectional
UTeM	-	Universiti Teknikal Malaysia Melaka

LIST OF SYMBOLS

%	-	Percent
°	-	Degree
cm3	-	Centimeter cube
g/cm3	-	Gram per centimeter cube
ϴ	-	Angle
Vf	-	Fiber volume fraction
Vm	-	Matrix volume fraction
Wf	-	Fiber weight fraction
Wm	-	Matrix weight fraction
ρ	-	Density
ρ_c	-	Lamina density
ρ_f	-	Fiber density
ρ_m	-	Matrix density
E_1	-	Lamina longitudinal modulus
E_f	-	Fiber elastic modulus
E_m	-	Matrix elastic modulus
v_{12}	-	In-plane Poisson's ratio
v_f	-	Fiber Poisson's ratio
v_m	-	Matrix Poisson's ratio
E_2	-	Lamina transverse modulus
ζ	-	Empirical parameter
G_{12}	-	Lamina in-plane shear modulus
G_f	-	Fiber shear modulus Gm - Matrix shear modulus.
G_{23}	-	Lamina out of plane shear modulus
σ_1	-	Maximum local stress along fiber direction
σ_2	-	Maximum local stress transverse to the fiber direction
τ_{12}	-	Maximum shear stress in the principal material direction
F_{1c}	-	Lamina longitudinal compressive strength

F_{mt}	-	Matrix tensile strength
F_{2c}	-	Lamina transverse compressive strength
F_{mc}	-	Matrix compressive strength
F_6	-	Lamina in-plane shear strength
F_{ms}	-	Matrix shear strength
α_σ	-	Standard deviation of fiber misalignment
V_v	-	Void volume fraction
Π	-	A constant with the value of 3.142

CHAPTER 1

INTRODUCTION

1.1 Background

The aircraft spoiler hinges are one of the important components in aircraft wing structure. The function of aircraft spoiler hinges is used as the helping mechanism to control and move the aircraft wing spoiler in order to slow and descend an aircraft. Moreover, the aircraft spoiler hinges also used to hold the panel of aircraft wing spoiler in a position in order to ensure the spoiler can properly function. It is to keep necessary lift and drag force which may receive any disturbances in open air environment at high altitudes such as loading of air and external force by vibration (Nasa, 2010).

Presently, the fast growing implementation composite material in aircraft has been seen include primary and secondary structure. The increasing usages of composite materials in aircraft structure due to high strength, stiffness and light weight. The composite material comprises the combination between reinforcement and matrix material embedded together to allow the material has a strength to change the direction of loading (Cairns, 2009). The polymer matrix composite such as fiberglass, carbon fiber and fiber-reinforced matrix systems are the common composite material used in aircraft structure. The decreasing weight of an aircraft by composite materials will save the fuel consumption of the aircraft. The composite materials in aircraft structure also less maintenance and repair costs compared to the metallic material because it does not easily corrode and crack from metal fatigue. (Houston, 2016).

There are many production methods of the polymer matrix composite in aircraft industries. The processes will depend on several factors such as cost, the shape of the component, the number of components and required performance. Typically, the production method of polymer composite can be related to the combination processes of two constituent such as polymer matrix and reinforcement. The method is involved assembling fiber, impregnating resin, forming product and curing the resin. In addition, the fabrication process of the composite in industries also can be divided into two methods such as open-face moulding and matched-die moulding. Open-face moulding is a method using only one mould, simple equipment and low-cost production while matched-die moulding required specific design moulding, complex tooling and equipment as well as more expensive production cost. Although, matched-die moulding fabrication method better in term of good finishing, closer control over tolerances and high production rate while open-face moulding depending on operator performance (Hoa, 2009).

1.2 Problem statement

Many aircraft spoiler hinges are still made from metallic material. For this research, the laminated composite plates are used as the main material of the spoiler hinge structure. Therefore, the composite spoiler hinges are still not well investigated in term of real condition testing in the laboratory. However, the composite material is heterogeneous and anisotropic in nature which required specific analysis and testing to investigate the hinges structurally. The load cases of existing spoiler hinge in the real condition operation are provided by Spirit Aerosystem. The existing aircraft spoiler hinges are subjected to the resultant force and the hinge moment due to a combination of air loading and the effect of wing deflections. The previous finite element method (FEM) result has shown that the composite aircraft is suffering some critical point due to the highest maximum stress concentration after subjected load cases (W. C. Mun, 2014). The real condition testing of the composite spoiler hinges in the laboratory is required to validate the finite element method (FEM) result.

1.3 Objectives

The objectives of this research are:

a) To develop jig for real condition testing in order to investigate structural of the composite aircraft spoiler hinge.
b) To compare and validate the finite element method (FEM) results by real condition experimental testing in the laboratory.

1.4 Scope

The scope of this research includes:

a) Literature study on the existing aircraft hinge design is provided by Spirit Aerosystem which includes determination loading applied to the structure of the hinge and working principle of existing metallic hinge spoiler. The study also on the related work of characteristic of the carbon fiber composite, jig design for testing machine and design an experimental test.

b) Designing a jig for the experimental test. This research involves designing a jig of testing machine respected to the real condition of existing aircraft spoiler hinge.

c) Developing a jig for the experimental test. This research involves the selection of appropriate material and the identifying strength of the jig.

d) Designing an experimental testing respect to the real condition of the existing aircraft spoiler hinge. This research includes a planning of the overall procedure, equipment and apparatus to running experimental test. It also includes the highlight important parameter, expected results and theoretical related to the experimental test.

e) Running an experimental testing on the aircraft composite spoiler hinge in the laboratory. This scope involves the running experimental testing with applying a tensile or compressive load on the specimen and collecting data of the experimental test result.

f) Analyzing result of experimental testing by comparing with the finite element method (FEM) result. This research involves a writing report in which analyzing the comparison and make the relation between experimental testing and FEM result.

CHAPTER 2

LITERATURE REVIEW

2.1 Composite

The composite material is a material formed with two or more combination of different material or constituents which mechanically act by each individual material or combination every single material behaviour (Gurdal Z., 1999; Mallick, 1997). The main feature of the composite material can be defined as very heterogenous and anisotropic material (Gay, 2014).

The composite can be classified into several types such as fiber, flake, particulate, laminar and filled composite. Fiber and Flake composite are made up from composed of chopped fiber and flat flakes while the Particulate composite is a composite made up from bonding of several particles. Moreover, the laminar composite is a composite made up from multi-layer of a constituent or ply while the Filled composite is made up from continuous skeletal matrix filled by the secondary material. The illustration types of composite materials shown in Figure 2.1 (Sierakowski, 2012):

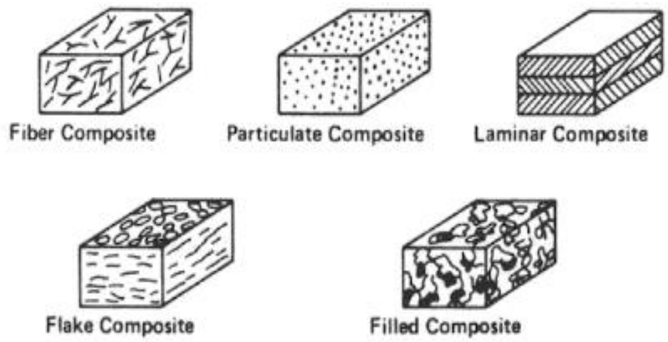

Figure 2.1: Illustration Types of Composite Materials (Sierakowski, 2012)

Basically, the concept of the composite is referred to bonding between constituents which known as matrix and reinforcement. Matrix is weak constituent embedded in composite but it acts as protection layer or keeps the arrangement of reinforcement. In another hand, reinforcement is harder, stronger and stiffer constituent than matrix which acts as the core of structural strength for the composite (Hull, 1996).

The combinations of two or more constituents developed a better material structure which the composite materials allow the matrix to transfer and distribute loads evenly to the reinforcements (Pandey, 2004). The matrix can be classified into several materials such as polymeric, ceramic, mineral and metallic matrix. The reinforcement also can be classified into several materials such as carbon fibers, glass fiber, organic fiber, boron fibers and etc (Chawla, 2012).

However, the creation of composite has started in thousand years ago by the ancient Egyptians to build their shelter. They built by using mud and straw which are embedded together to avoid shrinkage crack and to improve the tensile strength. This ancient idea is a source of inspiration to new development and inventions of composite materials. The origin idea development of composite material also initiates and influence by the existing nature around the human. Moreover, the bones also are the one good illustration composite origin notion which consists short and soft collagen fiber embedded in a mineral matrix called apatite (Chawla, 2012).

Presently, the composite material has been used in wide range of many industry sectors such as aerospace, automobile, boats, chemical, domestic, electrical and leisure (Gay, 2014). The growing demand for composite materials in industries influenced by needed requirement of industries to the material which has stiff, strong and light behaviour (A. Baker, 2004).

This reason has led to the highly growing of manufacturing light material but better strength such fiber composite. The development of composite material has shown significant improvement of mechanical properties over conventional metallic. The Figure 2.2 shown about the comparison between conventional monolithic metallic and composite materials in term of weight, stiffness, strength, fatigue resistance and thermal expansion (Chawla, 2012):

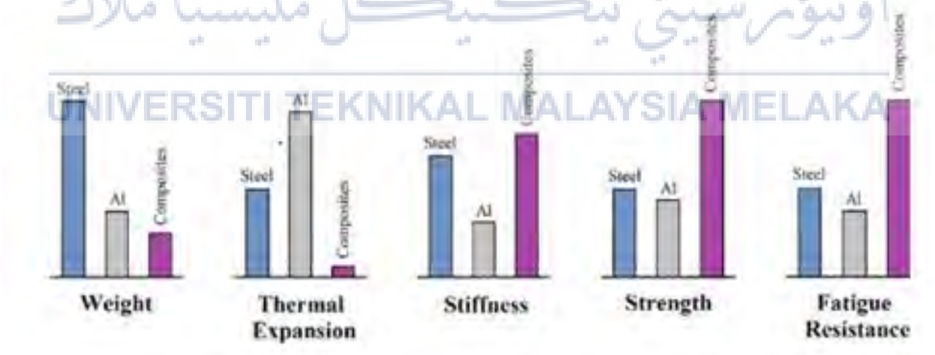

Figure 2.2: Comparison between Conventional Monolithic Metallic and Composite Materials.

(Chawla, 2012)

2.1.1 Laminated Composite

Laminated composite is also known as lamina or ply is an engineered material which made up from fiber-reinforced composite materials in form of multi-thin layers bonded together. (M. Abedi, 2015; Reddy, 2004). Laminated composite also contains a group of fibers held together by using a homogeneous matrix (Grandt, 2004).

The bonding between fiber and matrix material is strengthened by coupling agent or filler in order to increase toughness. The fiber in laminated composite also known as fiber-reinforced laminae which it can be classified into several types such as continuous or discontinuous, woven, unidirectional and bidirectional fiber-reinforced laminae. The various types of fiber-reinforced composite laminae are shown in Figure 2.3 (Reddy, 2004):

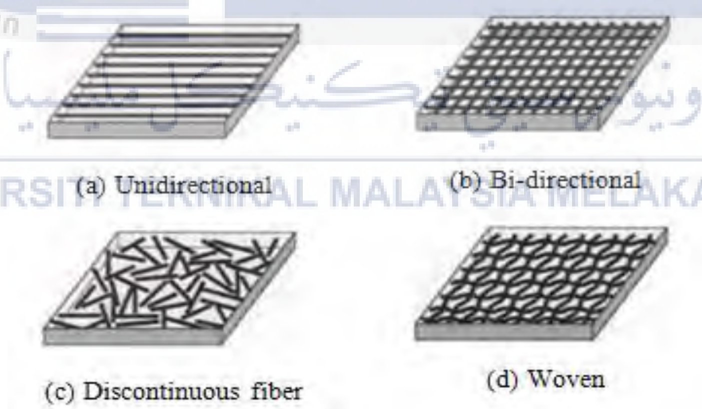

Figure 2.3: Types of Fiber-Reinforced Composite Laminae (Reddy, 2004)

The fiber-reinforced laminae are stacked together by multi-layer to form a laminate composite in order to accomplish stiffness and thickness. The sequence of the layers in a laminate is called the stacking sequence of lamination scheme (Reddy, 2004). The stacking of fiber-reinforced laminae may orientate in the same or different direction of fiber angle orientation of laminated composite (Kassapoglou, 2011). The most common fiber orientation in the laminated composite can be classified into several types such as a laminate with oriented laminae and laminate with cross-laminae.

A laminate with oriented laminae is a laminate composite has different fiber orientation where the orientation of each ply in the stacking sequence differ from its orientation in term of degree, θ relative to a reference axis such as between +90° and -90° for $0° \leq \theta \leq 90°$. The Figure 2.4 is a sample of a laminate with oriented laminae which the fiber orientation is 15/-30/0/90/45/-45 (Fantuzzi, 2014):

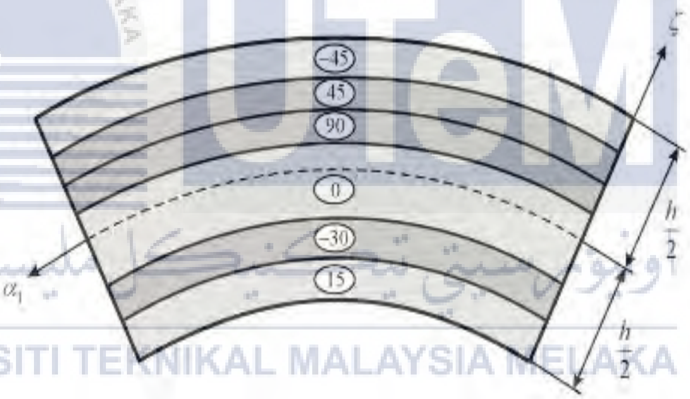

Figure 2.4: Laminate with Oriented Laminae (Fantuzzi, 2014)

Therefore, laminates with cross-laminae is a laminated composite has fiber orientation where the plies assume to be orientated at 0° or 90° for $0° \leq \theta \leq 90°$. Figure 2.5 is a sample of the laminates with cross-laminae which the fiber orientation is 0/90/90/0/0/90 (Fantuzzi, 2014):

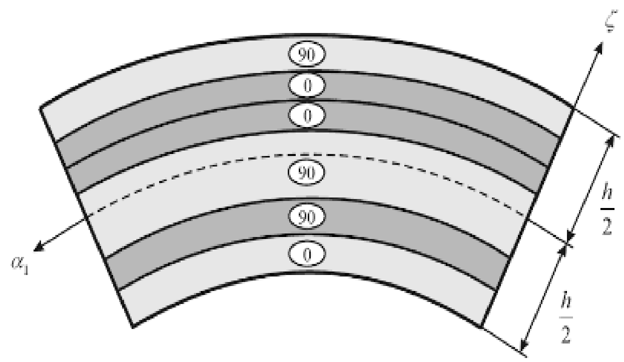

Figure 2.5: Laminates with Cross-Laminae (Fantuzzi, 2014)

2.1.2 Mechanics of Laminated Composite

The laminated composite has two mechanic studies which are micromechanics and macro-mechanics. Micromechanics is an analysis of composite material behaviour includes the study of the relationship between properties of the constituent in term of microscopic scale. The microscopic scale in the mechanic of laminated composite is exposed to investigation properties of the constituent internally structure in order to determine their effect to composite such as deformation and stress in the basic constituent of a structure. The effect of deformation and stress internally in basic constituents can be related to its stiffness and strength (Mukhopadhyay, 2005 ; Jones, 1998).

In order to determine properties of the laminated composite, the main factor of the composite which is density and relative proportion of fiber and matrix should be considered. The relative proportion of fiber and matrix can be related to weight and volume fractions of constituents. The following is the fraction of volume and weight for fiber and matrix (Mukhopadhyay, 2005 ; Barbero, 2011):

$$V_f = \frac{Volume\ of\ fiber}{Total\ Volume} \tag{2.1}$$

$$V_m = \frac{Volume\ of\ matrix}{Total\ Volume} \tag{2.2}$$

Where V_f is the volume fraction of fiber and V_m is the volume fraction of the matrix.

$$W_f = \frac{Weight\ of\ fiber}{Total\ Weight} \tag{2.3}$$

$$W_m = \frac{Weight\ of\ matrix}{Total\ Weight} \tag{2.4}$$

Where W_f is the weight fraction of fiber and W_m is the weight fraction of the matrix.

Moreover, the theoretical density of the lamina can be derived as follows:

$$\rho_c = \rho_f V_f + \rho_m V_m \tag{2.5}$$

Where ρ_c is the lamina density, ρ_f is the fiber density, ρ_m is the matrix density

Basically, the fiber in lamina is assumed as an orthotropic material. Moreover, micromechanics analysis in the laminated composite can determine five stiffness properties based on orthotropic material properties. The five stiffness properties of micromechanics analysis in laminated composite consists of longitudinal elastic modulus, transverse elastic modulus, in-plane Poisson's ratio, in-plane of the shear modulus and out of the plane of the shear modulus (Barbero, 2011).

Therefore, longitudinal elastic modulus of the lamina and in-plane Poisson's ratio can be indicated by using Rules of Mixtures (Barbero, 2011):

$$E_1 = E_f V_f + E_m Vm \tag{2.6}$$

Where E_1 is the lamina longitudinal modulus,

E_f is the fiber elastic modulus,

E_m is the matrix elastic modulus.

$$v_{12} = v_f V_f + v_m V_m \tag{2.7}$$

Where v_{12} is the in-plane Poisson's ratio,

v_f is the fiber Poisson's ratio,

v_m is the matrix Poisson's ratio.

Furthermore, the other stiffness properties of laminated composite such transverse elastic modulus can be obtained by using Halpin-Tsai equations as follows (Barbero, 2011):

$$E_2 = E_m \left[\frac{1 + \zeta\eta V_f}{1 - \eta V_f} \right] \tag{2.8}$$

$$\eta = \left[\frac{\left(\frac{Ef}{Em}\right) - 1}{\left(\frac{Ef}{Em}\right) + \zeta} \right] \tag{2.9}$$

Where E_2 is the lamina transverse modulus and ζ is an empirical parameter usually given the value of 2 for the case of circular or square fibers.

In addition, the lamina in-plane shear modulus is derived using cylindrical assemblage model (CAM) (Barbero, 2011):

$$G_{12} = G_m \left[\frac{(1+Vf)+(1-Vf)\,(Gm/Gf)}{(1-Vf)+(1+Vf)\,(Gm/Gf)}\right] \tag{2.10}$$

Where G_{12} is the lamina in-plane shear modulus,

G_f is the fiber shear modulus,

G_m is the matrix shear modulus.

Lastly, the lamina out of plane shear modulus can be computed using semi-empirical stress partitioning parameter technique (Barbero, 2011):

$$G_{23} = G_m \left[\frac{(Vf+\eta*)(1-Vf)}{\eta*(1-Vf)+(VfGm/Gf)}\right] \tag{2.11}$$

$$\eta* = \frac{3-4\,vm + (Gm/Gf)}{4(1-vm)} \tag{2.12}$$

Where G23 is the lamina out of plane shear modulus.

In Micromechanics analysis, the prediction strength of laminated composite can be determined only in rough estimation because the strength more accurate and better way determined through experimental. But rough estimation strength in micromechanics analysis is used due to the constraint of cost and time for fabrication and testing of lamina strength (Barbero, 2011).

The rough estimation strength in micromechanics analysis consists of the longitudinal tensile strength, longitudinal compressive strength, transverse tensile strength, transverse compressive strength, and in-plane shear strength of a lamina respectively (Barbero, 2011):

$$F_{2t} = F_{mt}\, C_v \left[\, 1 + \left(V_f - \sqrt{Vf}\right) \left(1 - E_m / E_f \right) \right] \tag{2.13}$$

$$F_{2c} = F_{mc}\, C_v \left[\, 1 + \left(V_f - \sqrt{Vf}\right) \left(1 - E_m / E_f \right) \right] \tag{2.14}$$

$$F_6 = F_{ms}\, C_v \left[\, 1 + \left(V_f - \sqrt{Vf}\right) \left(1 - E_m / E_f \right) \right] \tag{2.15}$$

$$X = \frac{G12\ \alpha\sigma}{F6} \tag{2.16}$$

$$C_v = 1 - \sqrt{\frac{4\,Vv}{\pi(\,1 - Vf)}} \tag{2.17}$$

Where: F_{1t} is the lamina longitudinal tensile strength,

F_{ft} is the fiber tensile strength,

F_{1c} is the lamina longitudinal compressive strength,

F_{2t} is the lamina transverse tensile strength,

F_{mt} is the matrix tensile strength,

F_{2c} is the lamina transverse compressive strength,

F_{mc} is the matrix compressive strength,

F_6 is the lamina in-plane shear strength,

F_{ms} is the matrix shear strength,

α_σ is the standard deviation of fiber misalignment,

V_v is the void volume fraction

Macromechanics of laminated composite is an analysis of composite material behaviour which focuses on the macroscopic effect. The material is assumed to be homogenous and orthotropic due to the effect of basic fiber and matrix material behaviour. In macro-mechanics, only the average properties of the lamina are used to expose macrostructural analysis of material by ignoring microstructure of lamina (Mukhopadhyay, 2005 ; Jones, 1998).

This study of Macro-mechanics analysis also provides information about loading acting on the laminated composite. The load applied on the laminated composite will exert in-plane or out-plane of principal direction of the lamina. Principal direction lamina also known as stress-strain relation axis occurs at properties along and perpendicular to the fiber direction. If the applied load acting the same direction with the fiber orientation, it provides adequate stiffness and strength to laminated composite materials (H. Altenbach, 2013).

The orthotropic behaviour of lamina allows the lamina to have high tensile and compressive strengths in the direction parallel to the fiber orientation. Therefore, fibers in a lamina are an orientation in the direction of the applied load and the laminas are stacked up to provide adequate stiffness and strength to the laminate. Laminated composite allows the optimization of material design but at the same time induced a complicated stress analysis (Reddy, 2004).

2.1.3 Failure in Laminated Composite

Generally, the laminated composite will be weak when the load is compressed due to matrix prevent longitudinal splitting and crack propagate parallel to fiber orientation (Steif, 1999). Multidirectional of laminated composite often suffered by compressive failure due to several failure mechanisms such as fiber kinking, fiber splitting, matrix cracking and delamination (Rofles, 2017; ZiaeRada, 2014).

Correlation between four failure mechanisms is the primary factor of ultimate failure in laminated composite (Rofles, 2017; ZiaeRada, 2014). Typically, these failure mechanisms can be observed by conducted experimental testing, even sometimes it difficult to see by naked eye. The failure terminology occurs inside the laminated composite also difficult and not well understands (ZiaeRada, 2014). The Figure 2.6 until 2.9 shows the illustration of compressive failure mechanism in laminated composite (ZiaeRada, 2014).

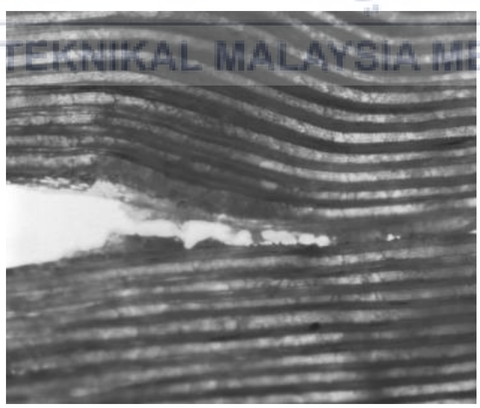

Figure 2.6: Fiber kinking (ZiaeRada, 2014)

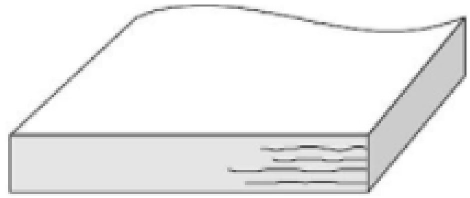

Figure 2.7: Fiber Splitting (ZiaeRada, 2014)

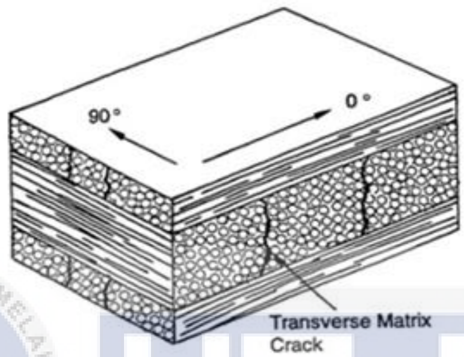

Figure 2.8: Matric cracking (ZiaeRada, 2014)

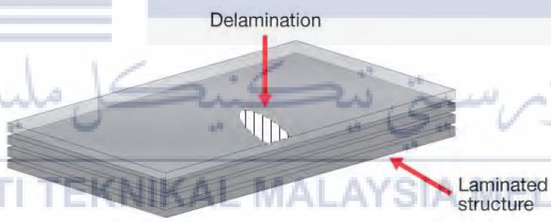

Figure 2.9: Delamination (ZiaeRada, 2014)

2.1.4 Composite in Aircraft Structure

The use of composite in design structural is rapidly growing in many industries especially in the aviation industry. The main reason increasing use of composite in aircraft structures due to reducing weight approximately between 10% and 30%, extremely high strength performance and saves the fuel intake. Composite material also superior fatigue properties and high corrosion resistance material which almost fulfil all design requirements need for aircraft structure (A. Baker, 2004; Paavola, 2015; Lewis, 1994).

In aircraft manufacturing industry, the usage of composite material has started in 1909 by first discovery of phenolic resin. The use of phenolic resin as the main composite material has been seen through manufacturing of deHavilland Albatross transport aircraft and deHavilland Mosquito fighter aircraft. The construction of deHavilland fuselage was manufactured from a ply-balsa-ply sandwich laminated using phenolic resin and wood (Groh, 2015; W. Roeseler, 2015). The fast growing commercial composite usage and development in composite structure has begun in the 1940s by several reasons such as requirement need for military vehicles, growing polymer industries, and extremely high theoretical strength but the light weight of composite materials (Holmes, 2011).

In the 1950s, the new development of composite materials such as carbon and glass fiber has moved composite material usage from military vehicles need to the commercial aircraft structure. The early commercial aircraft using composite material was through 707 and DC-9. However, the increasing use of composite material in commercial aircraft structure has been seen in late of the 1960s. The interior part sidewalls, bag racks, and galleys are successfully introduced and proved without causing harmful to the aircraft flying capabilities (W. Roeseler, 2015).

The transformation of secondary parts of commercial aircraft structure such as spoilers, rudders, ailerons, and flaps to carbon fiber composite was introduced in the 1970s. Although, The British Aerospace faced some challenges to prove the requirement need and to gain confidence level of authority. In addition, many interior parts and fairing of aircraft also were manufactured using fiberglass at that time (W. Roeseler, 2015).

The implementation of composite material in primary structures is most crucial and challenging time for designer and manufacturer. Until the 1980s, the primary structure like horizontal stabilizer has introduced by extensive testing and during fly evaluations through commercial aircraft 737. Furthermore, the first composite primary structures like vertical and horizontal stabilizer were successfully developed and manufactured in middle of the 1990s (W. Roeseler, 2015).

Presently, the almost entirely structure of aircraft has designed using high-performance carbon fiber composite including primary structure such as stabilizers, wings, and fuselage through commercial aircraft 787 Dreamliner. Figure 2.10 shows the primary and secondary structure of commercial aircraft 787 Dreamliner using various composite materials (W. Roeseler, 2015):

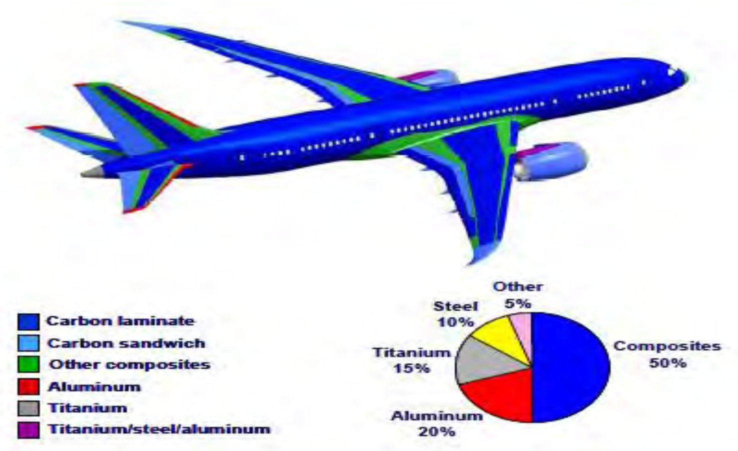

Figure 2.10: Commercial Aircraft 787 Dreamliner (W. Roeseler, 2015)

2.2 Aircraft Spoiler

The stability of an aircraft can be directly related to the control system. The controllability of an aircraft is important to ensure the safety of passengers during fly at high altitude. The mechanism is used to control an aircraft refer to control surfaces which can be classified as primary and secondary control surfaces. The primary control surface consists of the aileron, elevator, and rudder while secondary control surfaces consist of the flap, spoiler and tab. Figure 2.11 shows the classification of conventional control surfaces (Sadraey, 2014):

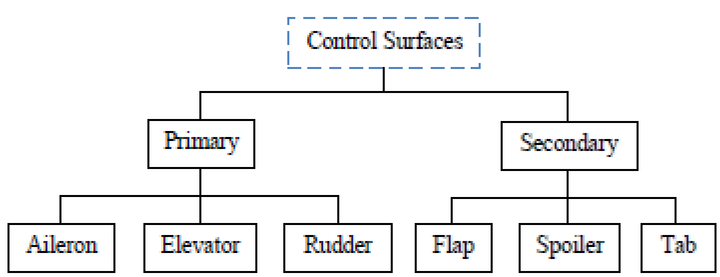

Figure 2.11: Classification of Conventional Control Surfaces (Sadraey, 2014)

However, the aircraft spoiler is one of the important components to control stability of an aircraft. Aircraft spoiler can be defined as the structure of rectangular plate or panel assembled and connected with fitting unit along the upper structure of aircraft wings (Nasa, 2010; Sadraey, 2014; Dawson, 2006). The illustration of position spoiler, flap, and aileron on aircraft wings has shown in Figure 2.12 (Sadraey, 2014):

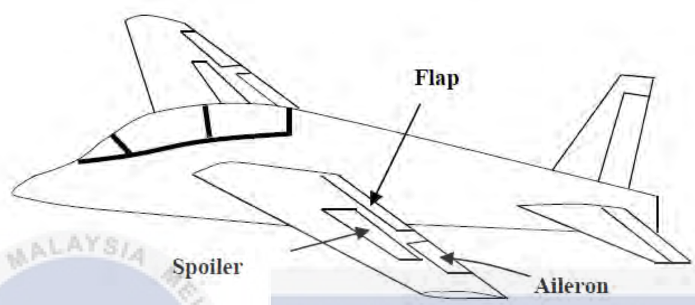

Figure 2.12: Position of Spoiler, Flap, and Aileron (Sadraey, 2014)

The aircraft spoiler consists of three primary functions such as to slow down during in-flight and landing, to move the aircraft at lower altitudes and to be a supporting mechanism for rolling control of an aircraft (Nasa, 2010; Sadraey, 2014; Dawson, 2006).

The spoilers also are working together with hinge bracket where the hinge moves the spoiler panel upward and downward in airstream boundary. (Nasa, 2010; Dawson, 2006). The working principle of spoiler is only to ensure the drag forces will increase while the lift forces will decrease in order to achieve the goals of function. Figure 2.13 shows the illustration of spoiler aerodynamic function (Sadraey, 2014):

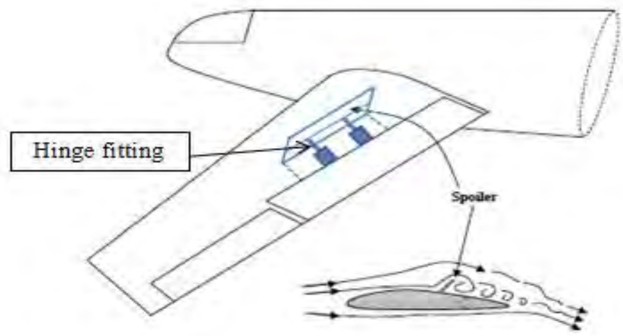

Figure 2.13: Spoiler Aerodynamic Function (Sadraey, 2014)

2.2.1 Aircraft spoiler hinges

Aircraft spoiler hinges also known as hinge fitting or hinge bracket of aircraft spoiler which it attached between spoiler and wings. The spoiler hinge is directly working together with spoilers which allow the spoiler move upward and downward in order to ensure working principle of spoiler is achieved. The spoiler hinge also is used to connect and hold the spoiler in position on top of aircraft wings which may receive disturbance by any external forces (W. C. Mun, 2014).

The external force exerted on the aircraft spoiler is due to the aerodynamic force. The force has concentrated at fitting linkage during in-flight at high altitude. The aerodynamic force acting on the spoiler also lies in various planes which it has developed bending moment in the area of hinges spoiler. However, the aerodynamic force and bending of the spoiler have influenced generating resultant force and moment at spoiler hinge. The Figure 2.14 is the illustration of the load acting on the spoiler (V.A. Komarov, 2015):

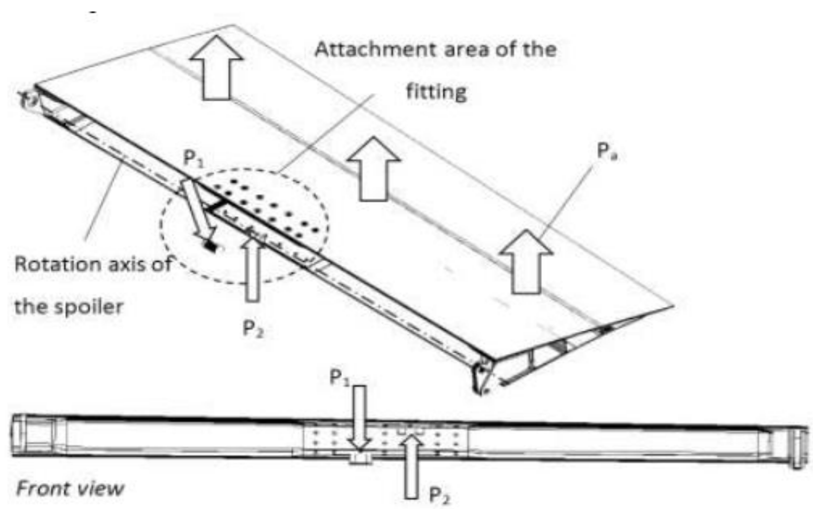

Figure 2.14: Loads Acting on Spoiler (V.A. Komarov, 2015)

However, the spoiler hinge has experienced stress concentration at certain area due to resultant force and hinge moment. The static analysis was conducted on existing metallic spoiler which the Von Mises stresses were found at the bolt, lug holes and sides surface of the hinge. The Figure 2.15 shows the stress distribution of metallic hinge spoiler for the close and open condition:

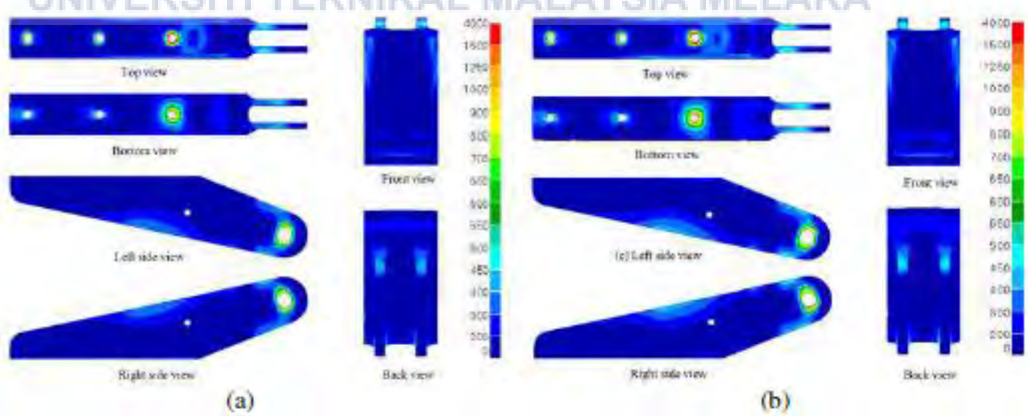

Figure 2.15: Stress Distribution of Metallic Hinge Bracket: (a) Spoiler Close; (b) Spoiler Open (W. C. Mun, 2014)

2.2.2 Aircraft composite spoiler hinges

The design of composite hinges spoiler has faced some challenge to transfer large concentration loading experienced by metallic to thin-walled layer. However, the mechanical properties of the laminated composite have calculated by using micromechanics formula (W. C. Mun, 2014).

Table 2.1: Mechanical Properties of Aircraft Composite Hinges Spoiler (W. C. Mun, 2014)

Longitudinal Modulus (MPa)	167480
Transverse Modulus (MPa)	23437
In-plane Poisson's Ratio	0.34
In-plane Shear Modulus (MPa)	5574
Longitudinal Tensile Strength (MPa)	3441
Longitudinal Compressive Strength (MPa)	5574
Transverse Tensile Strength (MPa)	100
Transverse Compressive Strength (MPa)	288
In-plane Shear Strength (MPa)	121
Density (g/cm3)	1.588

The strength analysis was conducted on composite hinge spoiler with respect to a primary parameter such as aerodynamic force, bending moment and deformation of spoiler. The result was indicated the highest concentration stresses obtained in a central area between two pairs of the lug. The Figure 2.16 shows the deformation and stress distribution of CAD model (V.A. Komarov, 2015):

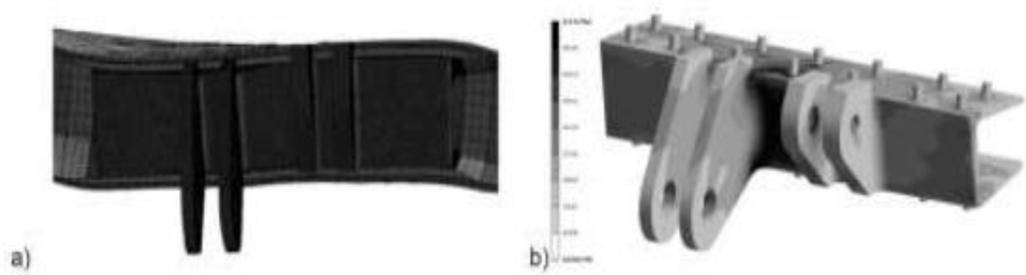

Figure 2.16: a) Deformation of CAD model b) Distribution force of CAD model.

2.3 Testing and Analysis

Mechanical testing can be defined as experimental work in order to determine mechanical behaviour and the functional of a specimen by exerted force in static or dynamic. The testing is able to indicate a material is safe and fulfil the requirement to use in specific applications (Joyce, 2008). The experimental testing on complex structure involves high difficulties analysis to be solved. However, it can be simplified using mechanical technique or principle such as superposition method. This method simplified a problem by explicit the problem by individual analysis and conclusion (Hopkins, 2004). Moreover, the analysis of a structure also can be referred to the analysis of failure criteria based on the behaviour of material either ductile or brittle. The failure analysis of the ductile material involved yielding criteria while brittle material involved fracture criteria under plane stress. Therefore, the failure criteria theory of brittle material is most interested in this research due to the composite spoiler hinges primarily in brittle.

2.3.1 Testing Machine

Testing machine is a device used to run the experiment as well as to measure mechanical behaviour and the functional of a specimen such as strength and deformation of the structure. The universal tester is a most typical machine used to investigate functional of the specimen. The machine is able to run in several conditions such as tension, compression and bending (ASM, 2004).

The control software of universal tester is helped the user to obtain the mechanical result such as a completed profile of force, extension against time, force against the extension, force against time, partial failure, slippage and percentage break. The speed test, value of force and extension of the experiment can be controlled by the user through the control software of machine (ASM, 2004).

However, the universal tester can be divided into two types of the testing machine such as electromechanical or hydraulic. An electromechanical machine is a machine dependent to electric speed motor by using a gear reduction system while hydraulic testing machine dependent whether one or two hydraulic pistons to move crosshead upward or downward. The main components of the hydraulic universal testing machine which are a frame, crosshead, load cell, table, and hardware and software control. The Figure 2.17 shows the illustration of the hydraulic universal testing machine (ASM, 2004):

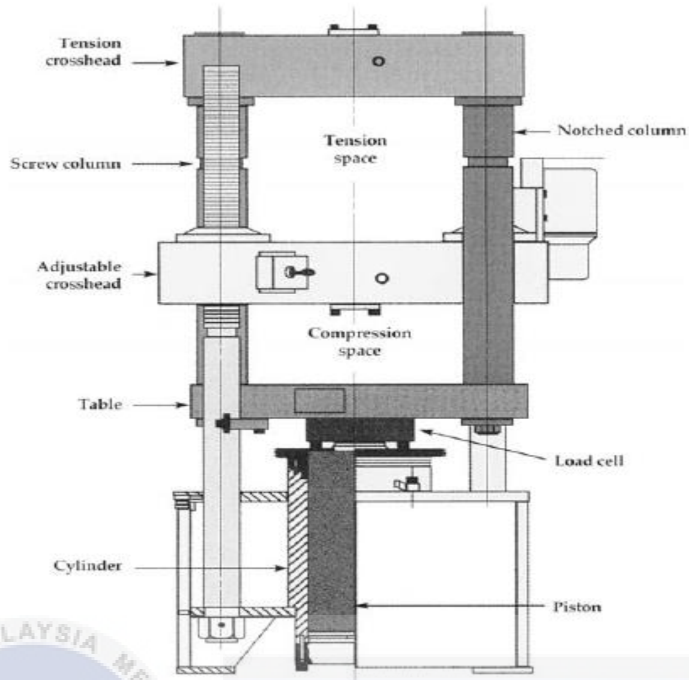

Figure 2.17: Components of a Hydraulic Universal Testing Machine (ASM, 2004)

2.3.2 Superposition Method

Superposition method is also known as superimpose method is a method of simplifying the complicated mechanical problem to easier analysis. The mechanical structure contains many loading or supported are very difficult to analyze especially in the real condition testing. This method also is used to minimize the error of harmonic frequency response sensitivity of the damped system and a thin sheet of metallic structure (W. Xiao, 2016; B. Wanga, 2016).

This method is separate the complicated problem of many loading or supported structure into a single analysis structure. This method can be illustrated through the complicated mechanical problem of deflection beams. Figure 2.18 has shown the illustration superposition method applied on a beam (Broutman, 1993; Hopkins, 2004):

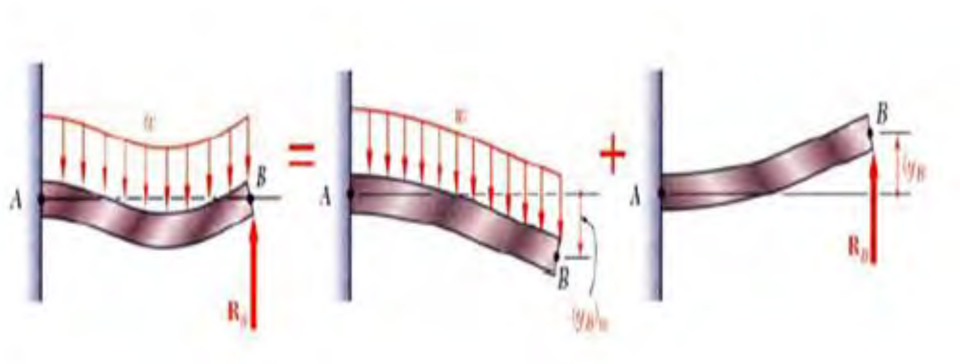

Figure 2.18: Superposition Method on Deflection of Beam (Broutman, 1993)

According to Figure 2.14, the analysis using superposition method is carried out by separate the load to the individual problem before combining the relation to conclude a final result. The method simplified the problem and equivalent to the whole structure analysis (Broutman, 1993).

2.3.3 Failure Criterion of Brittle Material

Generally, failure in the brittle material is involved suddenly rupture without yielding which crack propagate very rapidly. It also shows no region of plastic deformation as a warning before fracture. Therefore, ultimate tensile strength of the brittle material is a warning limit for working strength. There is two failure criterion in the brittle material which is maximum normal stress criterion and Mohr's failure criterion (Dewolf, 2011).

For maximum normal stress criterion, a brittle structure can be safe when principal stresses in the plane of stress which is maximum principal stress, σ_a and minimum principal stress, σ_b less than the ultimate strength of the structure as shown in Equation 2.18 and 2.19. This criterion also can be described by graphically which the structure will be safe when the value of σ_a and σ_b fall within square region ultimate strength plotting graph as shown in Figure 2.19 (Dewolf, 2011; Fenner, 2001)

$$|\sigma_a| < \sigma_{Ultimate\ Tensile} \quad (2.18)$$

$$|\sigma_b| < \sigma_{Ultimate\ compression} \quad (2.19)$$

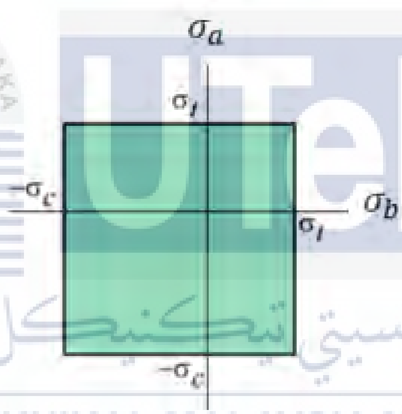

Figure 2.19: Rankine criterion failure (Fenner, 2001)

For Mohr's criterion failure, a brittle structure can be safe when ratio equation between principal stresses in the plane of stress (σ_a and σ_b) and ultimate strength ($\sigma_{Ultimate\ compression}$ and $\sigma_{Ultimate\ tensile}$) equal to or less than one. The ratio equation is written in Equation 2.20. This criterion also can be described by graphically which the structure will be safe when the value of σ_a and σ_b fall within square region ultimate strength plotting graph as shown in Figure 2.20 (Dewolf, 2011; Fenner, 2001)

$$\frac{\sigma_a}{\sigma_{Ultimate\ Tensile}} - \frac{\sigma_b}{\sigma_{Ultimate\ compression}} = 1 \qquad (2.20)$$

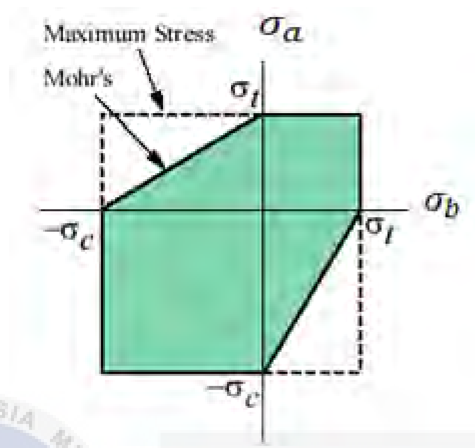

Figure 2.20: Mohr criterion failure (Fenner, 2001)

2.3.4 Deflection of Beam under Transverse Loading

The deflection of the beam under transverse loading is discussed about the analysis of the relationship between bending moment and deformation of a beam structure. Generally, pure bending within elastic range curve occur on a prismatic beam can be related to the distance of the bending arc circle, ρ, elasticity modulus, E and moment of inertia of cross section, I as shown in Equation 2.21 (Dewolf, 2011).

$$\frac{1}{\rho} = \frac{M}{EI} \qquad (2.21)$$

In order to determine the deflection of the beam at any point within elastic curve region, the Equation 2.21 is derived by using second order linear differential equation into the form of the deformed beam as shown in Equation 2.22 (Dewolf, 2011).

$$\frac{d^2y}{dx^2} = \frac{M}{EI} \qquad (2.22)$$

Based on Equation 2.22, the deflection of a beam can be analyzed by considering bending moment created from transverse loading, P and distance, x as shown equation 2.23 (Dewolf, 2011).

$$M = -\,Px \qquad (2.23)$$

The deflection Equation of elastic curve region is applied in order to investigate the relationship between bending moment and deflection under the elastic curve at any point. Therefore, the simple cantilever beam of the uniform cross section which experienced single transverse loading, P as shown in Figure 2.21 is used to derive the deflection equation of elastic curve region (Dewolf, 2011).

Figure 2.21: cantilever beam with single load at the end (Dewolf, 2011)

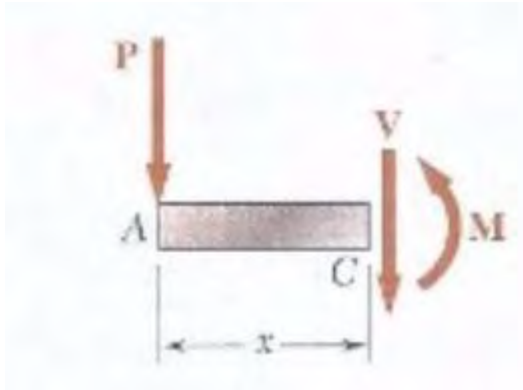

Figure 2.22: Free body diagram portion AC in distance of x (Dewolf, 2011)

According to Figure 2.21 and 2.22, the equation of deflection on the cantilever beam with a single load at the end within elastic curve region is governed by substituting M and multiplied EI in both directions of Equation 2.22 and then the equation 2.22 is integrated into a term of x-direction. By solving several constants of integration, the equation of deflection on the cantilever beam with a single load at the end within elastic curve region is developed as shown in Equation 2.23 below (Dewolf, 2011).

$$y = \frac{P}{6EI}(-x^3 + 3L^2x - 2L^3) \qquad (2.24)$$

Where y is a deflection of the beam, P is transverse loading, E is elasticity modulus, L is the total length of beam and x is the distance from any location between high bending moments occurred. By letting x is equal to zero, the deflection at the end of the beam can be derived in Equation 2.24 below (Dewolf, 2011).

$$y = -\frac{PL^3}{6EI} \qquad (2.25)$$

CHAPTER 3

METHODOLOGY

3.1 Introduction

The planning activities in order to achieve objectives of the research are presented in this chapter. The activities are respected to the time constraint of two semesters. This chapter provides the work flow of research journey includes finding of related information, taking a measurement of related variables, developing new custom jigs for testing and running the experiment. Figure 3.1 shows the flow chart of the research journey:

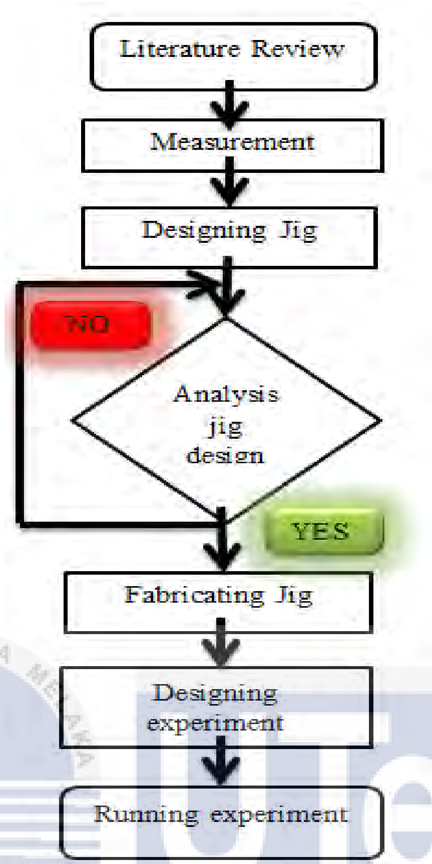

Figure 3.1: Flow Chart of Research Journey

3.2 Working Method for Design Testing

A new working method to validate the previous result of the finite element method (FEM) is presented in this chapter. This method is emphasized on the experimental testing which conducted in a laboratory which mimics the real condition. The loading cases exerted on the existing spoiler hinge in the real condition are provided by Spirit Aerosystem. Therefore, the force and the hinge moment are determined to be subjected at the lug holes of the spoiler hinge at the same time by 4684 N and 7310 Nm respectively.

However, the testing machine in the laboratory has a limitation where the force and the hinge moment cannot be exerted at the same time on the specimen. The superposition method is introduced to solve the problem which divided the testing into two experiments. Figure 3.2 show the illustration of superposition method applied at spoiler hinge design:

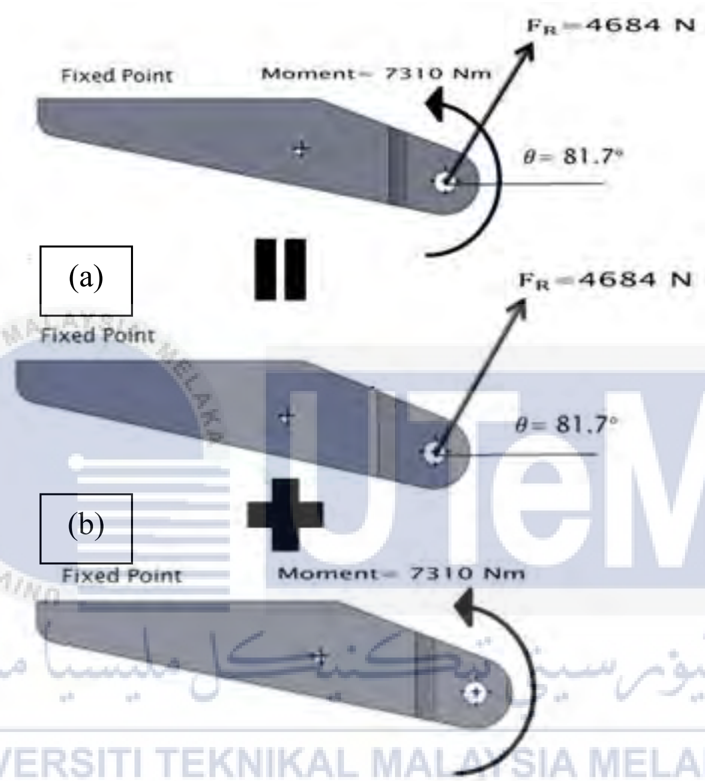

Figure 3.2: Illustration of Superposition Method

Figure 3.2 illustrates the visual idea of superposition method applied at composite spoiler hinge. The same hinge is tested separately by force and couple moment in two experiments but the test still equivalent to mimic the real condition. These two experiments are called as testing for resultant force and testing for the hinge moment. These testing have a constraint to consider which are fixed point at holes of the bolt and loading point (force and couple moment) at holes of lug composite spoiler hinge. The superposition method is used as a solution for testing machine limitation and this method also influenced to the development of the new custom jig design. The two experiments are required several new custom jig design to install with specimen and machine in order to conduct the testing.

3.3 Development of Custom Jig for Experimental Testing

The new custom jigs are developed with respect to the existing jig design and the related component which installed and assembled together during the experiment. Besides that, the new custom jig designs also worked together with the specimen and universal testing machine in order to mimic the real condition. Figure 3.3 is shown the flow of development custom jig.

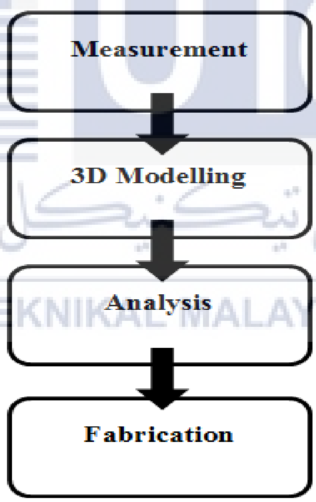

Figure 3.3: Steps of Development Customized Jig

The existing jig, specimen and the related component such as the extension jig and the universal testing machine are measured in the first step for generation idea of custom jig development and dimension constraint for new designs of the custom jig. All components and parts are involved in measurement process shown from Figure 3.4 until 3.7.

Figure 3.4: Composite Spoiler Hinge (Specimen)

Figure 3.5: Housing jig

Figure 3.6: Existing Jig

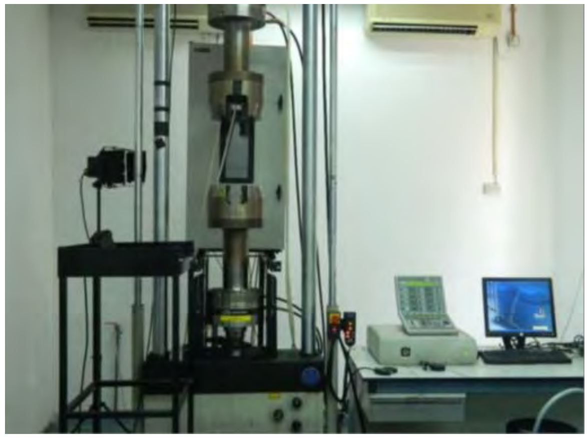

Figure 3.7: Universal testing machine

In the second step, the four models of the custom jig are designed where the one of model design is for resultant force testing and other three model designs are for hinge moment testing. All jig designs are developed using SolidWork software in order to give a visualization of fully image and dimension for further process. The model of a custom jig used in testing for resultant force is named as a jig for the resultant force as shown in Figure 3.8.

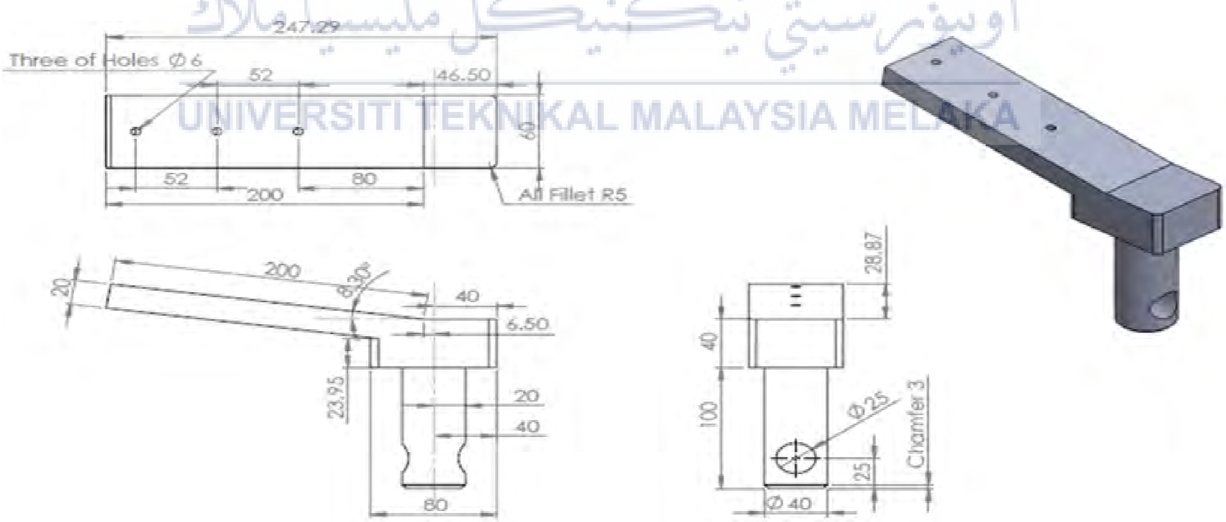

Figure 3.8: Design of Jig for Resultant Force

Moreover, the three model of custom jigs used in testing for hinge moment are named as upper and lower jig for hinge moment, couple moment connector and fixed support as shown in Figure 3.9 until 3.11

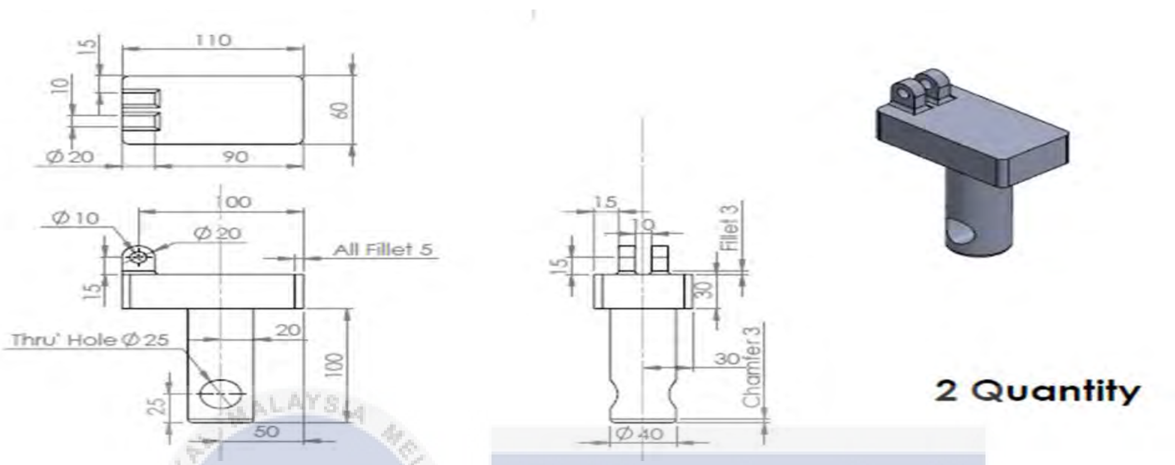

Figure 3.9: Design of Jig for Hinge Moment

Figure 3.10: Couple Moment Connector

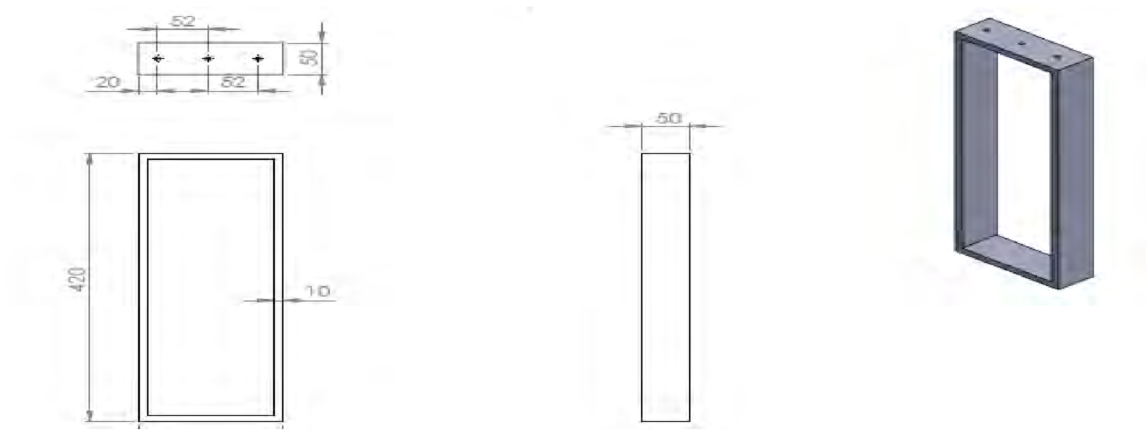

Figure 3.11: Fixed Support

For the third step, the models of the custom jig are analyzed by using Finite Element Analysis (FEA) approach. This approach is used to analyze the structure of the custom jig when the load is applied during the experiment. The analysis of the model is respected to the three stages of FEA approach which are preliminary analysis, discretization and boundary condition before obtaining the result. The Figure 3.12 is shown stages of FEA Approach.

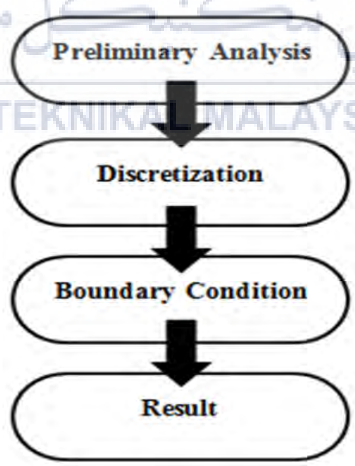

Figure 3.12: Stages of FEA Approach

As shown in Figure 3.12, the preliminary analysis is the first stage of Finite Element analysis approach which consists of the identifying the nature of material properties of geometry model. The structure of the jig model is assumed to be isotropic homogeneous metallic material due to the material used is mild steel. At the second stage, the generating mesh of the model is involved by divided into several small elements. Therefore, all elements are related each other by connection of nodes. The every point of nodes in the mesh is used to determine stresses experienced by a model which investigate the relationship between force and extension of the model. This stage has known as discretization.

Furthermore, the boundary condition is the third stage of FEA approach. At this stage, the fixed point and applied load of the jigs model are introduced. The fixed point is located on holes of the bolt while applied load is located on the hole of the lug. After that, the result is obtained at last stage of FEA Approach in term of the maximum Von-Mises Stress and total deformation. The purpose analysis of custom jig models identifies the requirement of design is satisfied where the model of the custom jig does not extremely deform and break after subjected loading during the testing.

For the last step of custom jig development, the fabrication processes of the custom jig are conducted after analyzed result of finite element method which shown the acceptable result. The mild steel material is used as the main material of the custom jigs due to cheaper cost and suitable working strength as a jig. Moreover, fabrication processes also are respected to the dimension provided in CAD drawing of custom jig model as shown from Figure 3.8 until 3.11. The process of fabrication is involved several some manufacturing processes such as lathing, milling, welding, grinding and threading.

3.4 Experimental setup

The testing in the laboratory to the mimic real condition of spoiler hinge operation is divided into two experiments. The first experiment has known as testing for the resultant force which it involves applying the force in certain direction angles at the lug of the specimen. Furthermore, the second experiment has known as testing for the couple moment which it involves applying couple moment at the lug of the same specimen.

The both testing is conducted in order to investigate weak point as well as to validate previous FEM result. The aircraft composite spoiler hinge as the specimen of this research has made up from IM7/8552 laminated composite plates. The equipment and machine are directly involved in two experiments which are the universal testing machine, extension of jigs and custom jigs of testing. The general procedural information for the both experiments can be divided into several steps has shown in Figure 3.13:

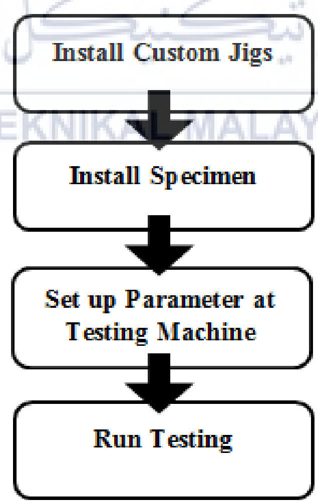

Figure 3.13: General Experimental Procedure

3.4.1 Setup of Testing for Resultant Force

Testing for resultant is a testing respected to the first condition of superposition method which the resultant force at certain direction is exerted on the lug hole of the hinge. However, the testing also respected to the real condition constraint of hinges which is fixed point occur on the holes of bolt and loading point occur on the hole of the lug. The Figure 3.14 is shown a 2D illustration of the first experiment condition.

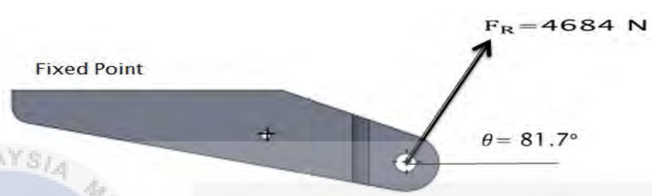

Figure 3.14: 2D illustration of the first experiment condition.

Based on, the first testing is conducted by using a certain combination of several jigs and another component in order to create a resultant force at certain direction on the specimen. The jigs and other component are involved such as jig for resultant force, standard existing jig, extension jigs, bolt, and nut as shown from Figure 3.15 until 3.18.

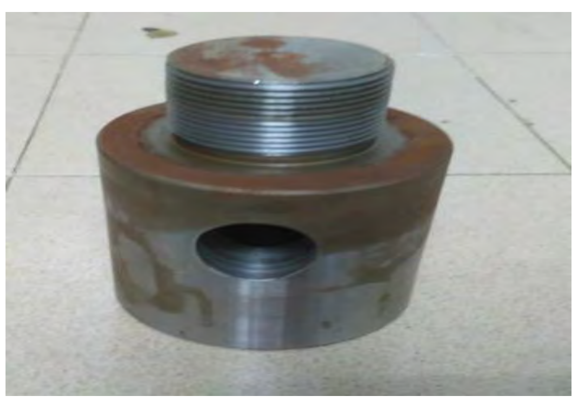

Figure 3.15: Extension jig

Figure 3.16: Jig for resultant force

Figure 3.17: Standard existing jig

Figure 3.18: Bolt and nut

The setup of testing for resultant force is beginning by the installation of extension jig on the threading holes of upper and lower crosshead of the universal testing machine. The installation extension jig on the testing machine is shown in Figure 3.19.

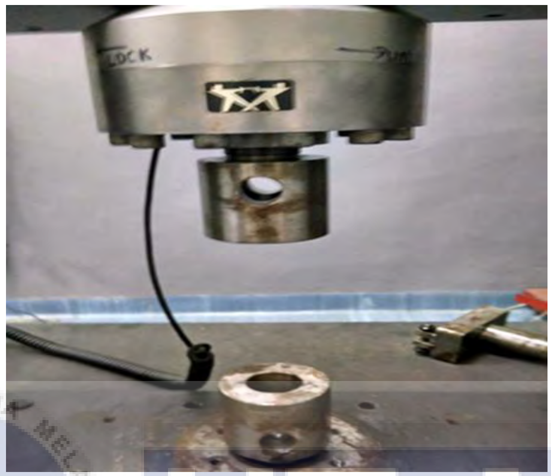

Figure 3.19: Installation extension jig

After that, jig for resultant force and standard existing jig are installed on the both extension jig at crosshead of the machine and locked by cylinder block in the slot. In addition, the fixed point of the specimen which is the holes of the bolt is installed on the jig for resultant force and loading point of the specimen which is the hole of the lug is installed on the standard existing jig. The installation specimen and custom jig of testing for resultant force are shown in Figure 3.20.

Figure 3.20: Installation specimen on custom jig of testing for resultant force

On the next step, the control parameter such as applied load and speed of crosshead are set up through the control software of the machine. The loading and crosshead speed of testing for the resultant force which is 2 mm/min and 4.7 kN. Last but not least, the testing is running until the load case for the resultant force testing is reached. The specimen is physically observed and measurement data of testing is collected for further interpretation.

3.4.2 Setup of Testing for Hinge Moment

Testing for hinge moment is a testing respected to the second condition of superposition method which the couple moment is exerted on the lug hole of the hinge. However, the testing also respected to the real condition constraint of hinges which is fixed point occur on the holes of bolt and loading point occur on the hole of the lug. The Figure 3.21 is shown a 2D illustration of the second experiment condition.

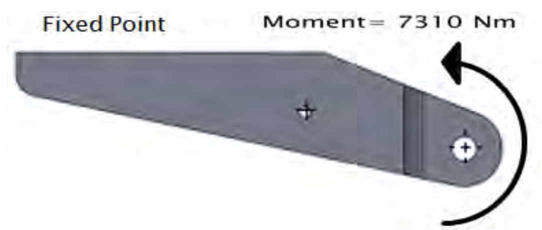

Figure 3.21: 2D illustration of the second experiment condition.

According to Figure 3.21, the second testing is conducted by using a certain combination of several jigs and another component in order to create couple moment on the specimen. The extension jig, bolt and nut as shown in Figure 3.15 and 3.18 also used as a similar function in the second testing. However, the usage of custom jigs is different for the second testing which is three custom jig are involved such as couple moment connector, fixed support and jig for hinge moment as shown from Figure 3.22 until 3.24.

Figure 3.22: Couple moment connector

Figure 3.23: Fixed Support

Figure 3.24: Jig for Couple Moment

The setup of Testing for Hinge Moment also begins by the installation of extension jig on the threading holes of upper and lower crosshead of the universal testing machine. The installation process of extension jig is similar in the first testing as shown in Figure 3.19. After that, jig for hinge moment is installed on the both extension jig at crosshead of the machine and locked by cylinder block in the slot.

In addition, the fixed point of the specimen which is the holes of the bolt is installed on the fixed support jig. Moreover, the couple moment connector is installed between loading point which is the hole of lug and jig for couple moment. All connection is locked by using bolt and nut. The installation of the specimen on the custom jig is shown in Figure 3.25.

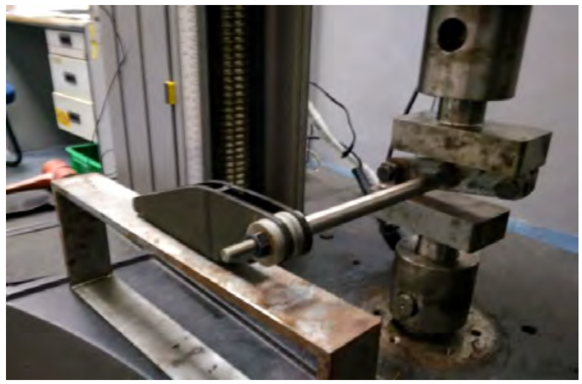

Figure 3.25: Installation specimen on the custom jig of testing for hinge moment

On the next step, the control parameter such as applied load and speed of crosshead are set up through the control software of the machine. The loading and crosshead speed of testing for couple moment which is 2 mm/min and 61 kN. Last but not least, the testing is running until the load case for the hinge moment testing is reached. The specimen is physically observed and measurement data of testing is collected for further interpretation.

Unfortunately, the testing for hinge moment experienced a problem due to the custom jig of couple moment connector is slipped when the load is applied. The result of testing for hinge moment is not really accurate and not relevant to interpret due to the slipping between the jig and specimen. However, the student has taken an alternative to analyze the specimen by conducted compression test. The setup of the compression test is similar to the testing for resultant force as shown in Figure 3.20 but the load is applied until specimen fails

CHAPTER 4

RESULT AND DISCUSSION

4.1 Analysis of Custom Jig Model

The static analysis of four custom jig models is conducted by using ANSYS software. The result of graphical colouring zones, equivalent von-misses stress and total deformation of the models are obtained with respect to the four stages of Finite Element Analysis approach such as preliminary result, discretization, boundary condition and result.

The mild steel material is used as the main material of all models where its density, young modulus, yield strength and Poisson's ratio is 7800 $\frac{\text{kg}}{\text{m}^3}$, 210 GPa, 250 MPa and 0.3 respectively. The automatic method is used as discretization of generating a mesh for all models because this analysis only to obtain rough estimation result before fabrication process. The Figure of 4.1 until 4.4 shows the graphical colouring zones of stress distribution and deformation for all custom jig models:

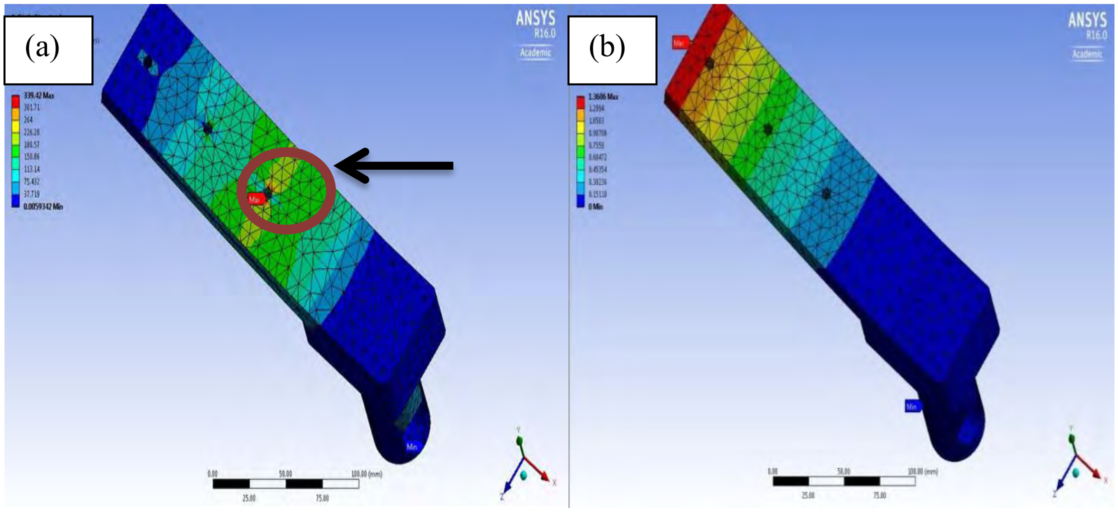

Figure 4.1: (a) Stress distribution and (b) Deformation of Jig for Resultant Force

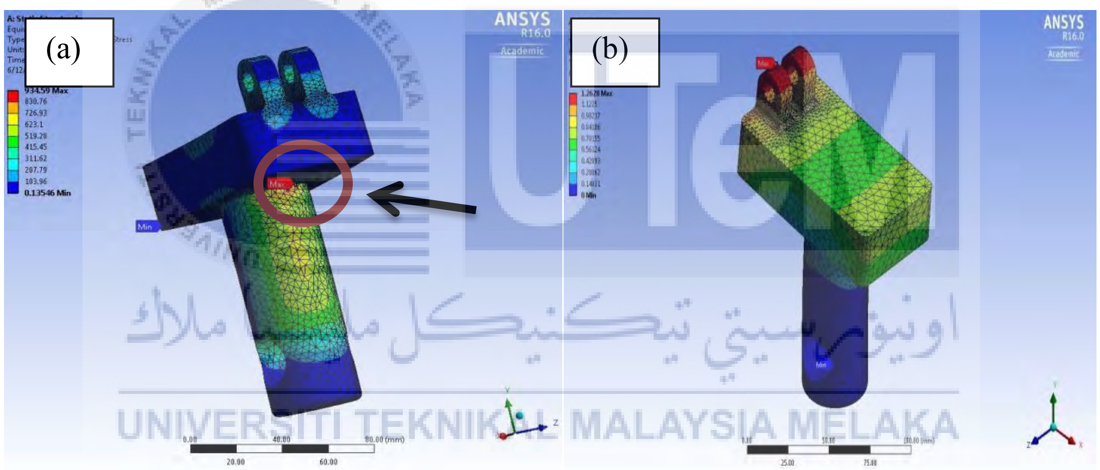

Figure 4.2: (a) Stress distribution and (b) Deformation of Jig for Couple Moment

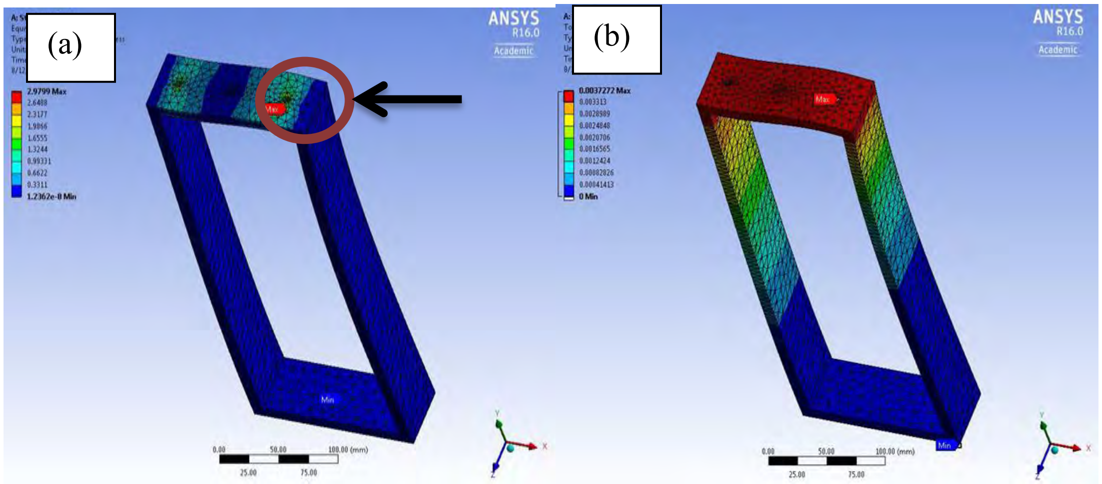

Figure 4.3: (a) Stress distribution and (b) Deformation of Fixed Support

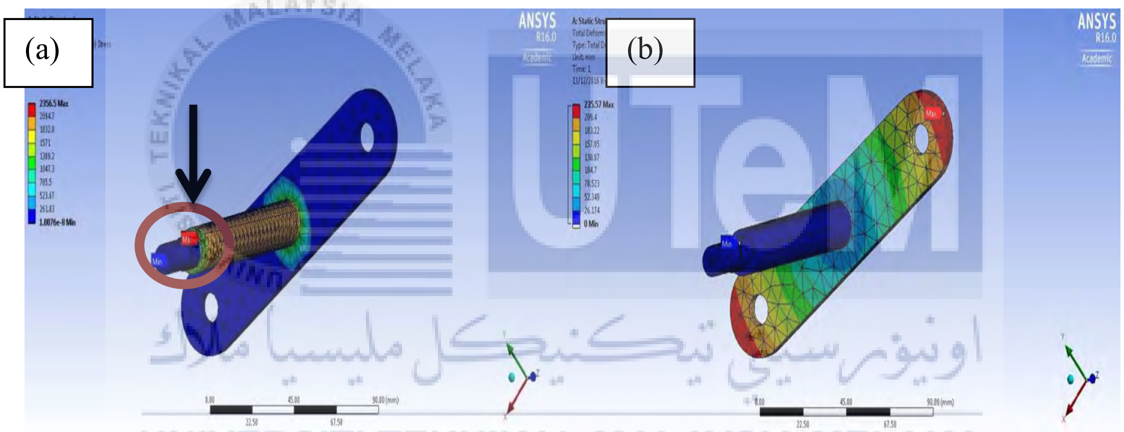

Figure 4.4: (a) Stress distribution and (b) Deformation of Couple Moment Connector

Furthermore, the result of Finite Element Analysis in term of maximum equivalent Von-Misses and total deformation for all custom jig models are tabulated in Table 4.1:

Table 4.1: Result of Finite element analysis of custom jig models

Custom Jig	**Maximum equivalent Von Misses stress (MPa)**	**Total deformation (mm)**
Jig for Resultant Force	339.42	1.361
Jig for Couple Moment	934.59	1.263
Fixed Support	2.98	0.003
Couple Moment Connector	2356.3	235.57

The custom jig model of fixed support as shown in Figure 4.3 is only one model shown the small value of maximum equivalent Von-misses stress and total deformation which is 2.98 MPa and 0.003 mm respectively. So that, this custom jig model is safe to be fabricated. According to Figure 4.1, Jig for Resultant Force experienced the high value of maximum equivalent Von-misses stress which is 339.42 MPa in a small region where it occurred inside the hole. However, the jig model is considered to be safe for fabrication due to coarse mesh inside the holes which give the rough estimation result and show the only small area of warning red colour contour of stress distribution.

Based on Figure 4.2 and 4.4, jig for hinge moment and jig of couple moment connector are also acceptable for fabrication because the highest maximum stress which is 934.59 MPa and 2356.3 MPa which only occurred at the cleavage of the model in the small region. The reason of high maximum stress due to the calculation of coarse mesh at cleavage only gives rough estimation result. The model also shows least warning red colour contour of stress distribution and almost entire model in blue colour contour which means the structure of the model still in good condition.

4.2 Experimental Result of Aircraft composite spoiler hinges

Experimental testing of Aircraft composite spoiler hinges in the laboratory is tried to mimic the real condition of aircraft operation. In addition, the testing is focused only on the highest load cases which provided by Spirit Aerosystem. Spirit Aerosystem also provided the real condition of aircraft operation which the hinges are suffered by two loading which is a resultant force and hinges moment. However, the limitation of the tester machine in laboratory influenced the dividing of testing into two experiments which are testing for resultant force and testing for hinge moment. Furthermore, the conducting two experiments also are supported by theoretical literature information of superposition method as mention in Chapter 2.3.2.

The result of testing for resultant force is obtained after applied compressive load on hinges at specific custom jigs. The loading in range 0 kN until 4.7 kN is applied on hinges by three times. Figure 4.5 showed the force versus extension curve of testing for the resultant force which it developed after the loading reached 4.7 kN. The experimental result of testing for resultant force is tabulated in Table 4.2 below.

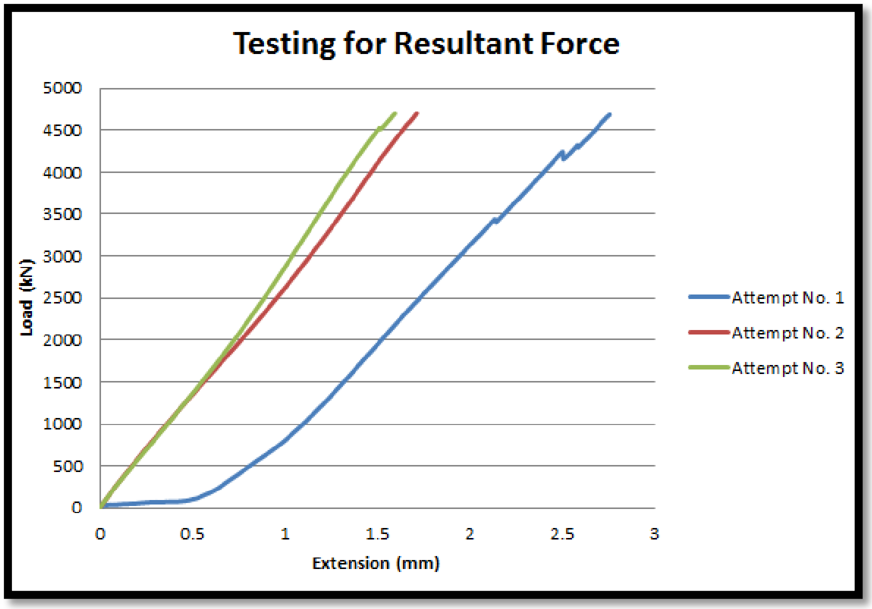

Figure 4.5: Force versus Extension Curve of Testing For Resultant Force

Table 4.2: Experimental Result of Testing For Resultant Force

Attempt Test No.	Maximum Load (kN)	Compressive Stress at Maximum Load (MPa)	Compressive Strain (Extension) at Maximum Load (mm/mm)	Compressive Extension at Maximum Load (mm)
1	4.7	3.92	0.06	2.75
2	4.7	3.92	0.03	1.71
3	4.7	3.92	0.03	1.59
		Average :	0.04	2

According to Figure 4.5, the three attempt of the testing for resultant force are showed the linear curve and directly proportional relationship between loading and extension of the hinge. Based on Table 4.2, Compressive stress, strain and extension are obtained when the maximum loading of 4.7 kN is reached. The compressive stress at maximum load of all three attempts has presented the value of 3.92 MPa. Besides that, compressive strain and extension at maximum load are showed a slightly different value between three attempts. The average value of compressive strain and extension at maximum load are presented by 0.04 mm and 2 mm respectively.

For the second experiment which is testing for hinge moment, the tensile load is applied through the several specific custom jigs in order to create couple moment on the hinges. The force versus extension curve of testing for hinges moment is showed in Figure 4.6 below.

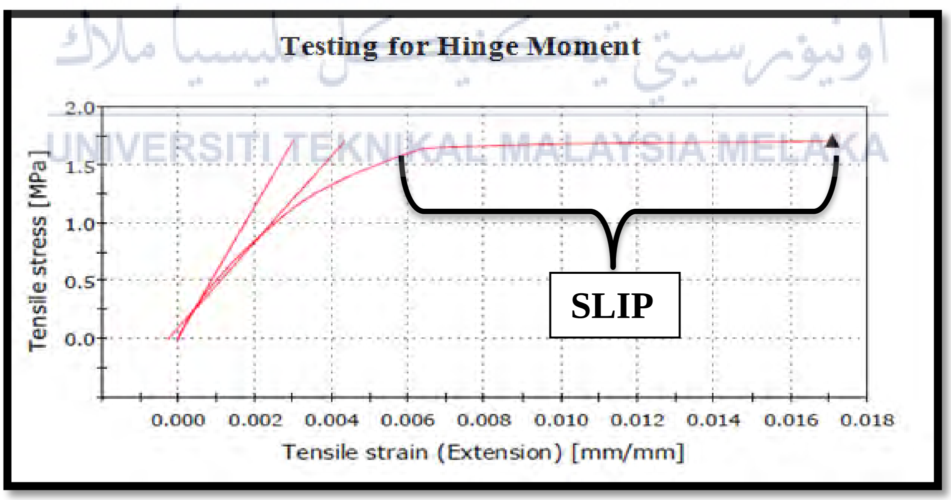

Figure 4.6: Force versus extension curve of testing for hinges moment

According to the Figure 4.6, the result of the testing for hinge moment is showed the curve increase linearly within range 0 MPa until 1.71 MPa of tensile stress. After that, the curve is started to be a constant line at 1.71 MPa of tensile stress. The constant line curve phenomena occurred due to slipping between the holes of hinge and custom jig during the experiment. Unfortunately, the result of testing for hinge moment is not really accurate and not relevant to interpret due to slipping between specimen and custom jigs.

However, several actions are carried out to solve the problem by installed washer between hinges and customs jig but the slipping phenomena still occurred. In addition, the design of the slipping custom jig also cannot be improved due to the limitation of time and cost. Therefore, the student has taken an alternative to conducting the compression test by advising from a supervisor. The result of compression test is used to validate and compare with the result of finite element method.

The compression testing is conducted by applying a compressive load of 10 kN with three times attempted but the specimen started to fail at the second attempt by a load of 3.9 kN. The curves of load versus extension for all attempt of compression testing are shown in Figure 4.7 and 4.8. All attempt experimental result for compression testing of Aircraft composite spoiler hinges is tabulated in Table 4.3 below.

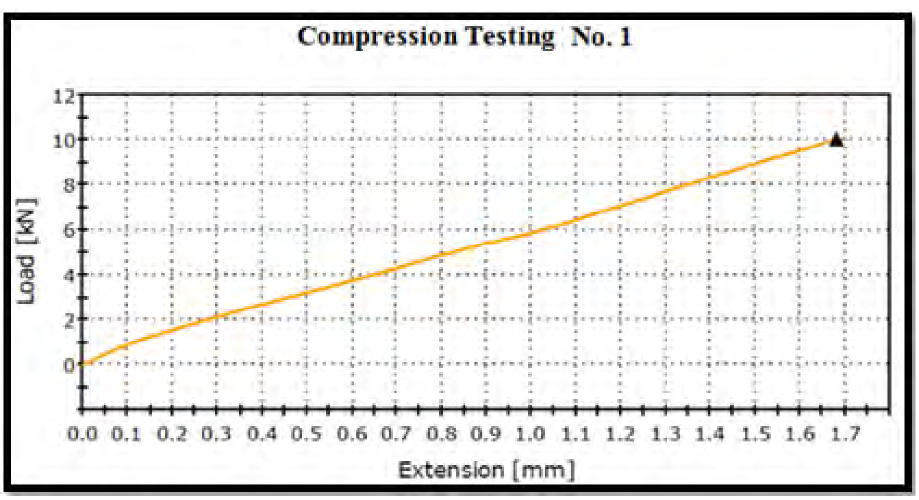

Figure 4.7: Curve of Load versus Extension of Compression Testing for Attempt No. 1

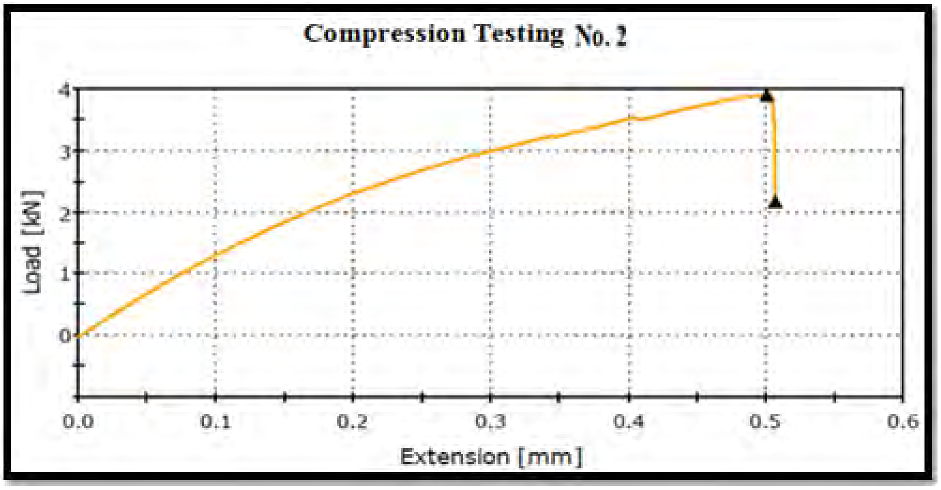

Figure 4.8: Curve of Load versus Extension of Compression Testing for Attempt No. 2

Table 4.3: experimental result for compression testing of Aircraft composite spoiler hinges

Attempt Test No.	Maximum Load (kN)	Compressive Stress at Maximum Load (MPa)	Compressive Strain (Extension) at Maximum Load (mm/mm)	Compressive Extension at Maximum Load (mm)
1	10	16.67	0.03	1.68
2	3.9 (Fail)	6.49	0.01	0.5
3	-	-	-	-

Last but not least, the structural of aircraft composite spoiler hinge is analyzed by comparing the result of compression testing and finite element method. The result of finite element method (FEM) provided by the engineer of CTRM is used to compare with the theoretical and experimental result. All result will be compared in order to investigate hinges structural in term of deflection and physical analysis.

4.2.1 Structural Analysis of Aircraft composite spoiler hinges

Firstly, the deflection of aircraft composite spoiler hinges is analyzed by comparing three points of the linear curve of first attempt experimental deflection with theoretical calculation deflection. The theoretical calculation deflection is calculated with respect to the theory of deflection of the beam as a review in Chapter 2.3.4. Figure 4.9 is shown the relationship between deflection of beam and deflection on hinges.

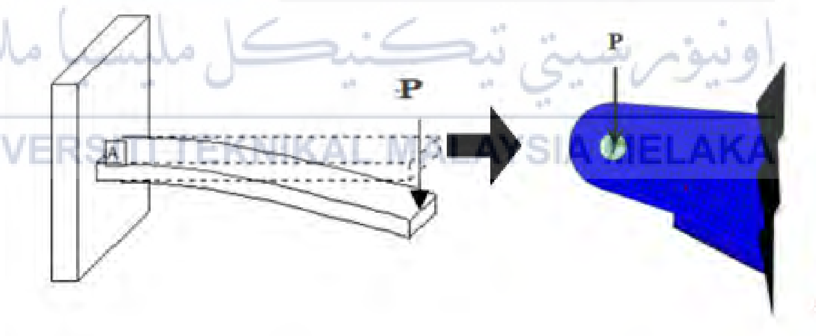

Figure 4.9: Relationship between deflection on beam and deflection on hinges

For related to the deflection of beam theory, the aircraft composite spoiler hinges is considered as simple cantilever beam under single transverse loading at the end and uniform cross section as shown in Figure 4.9. Therefore, the Equation 2.24 is used to calculate the theoretical deflection of three points on first attempt linear curve of compression testing as shown in Figure 4.10 below.

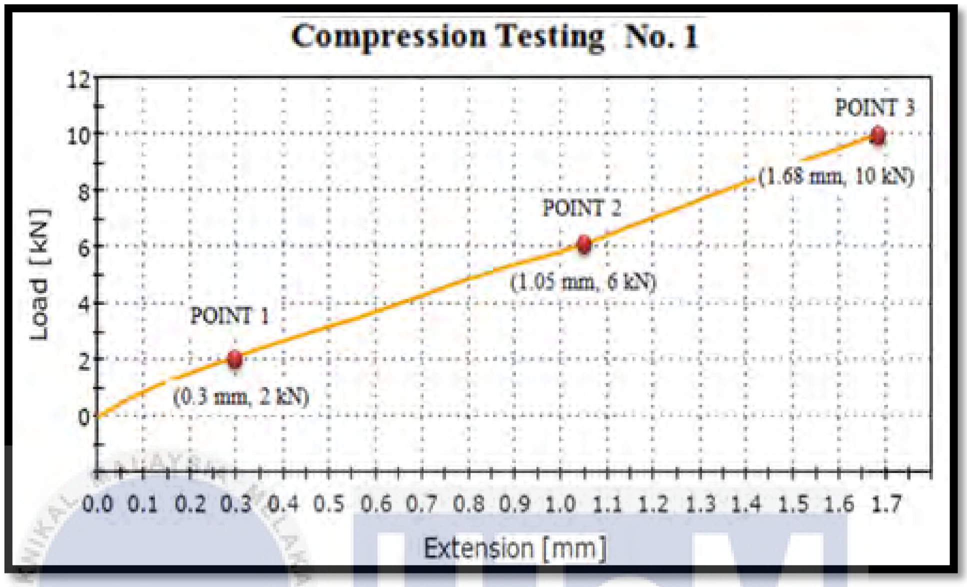

Figure 4.10: Three point deflection analysis between theoretical and experimental

According to Figure 4.9, the theoretical deflection is calculated based on the load of points 1, 2 and 3 which are 2 kN, 6 kN and 10 kN using Equation 2.24 and the value of theoretical deflection will be compared to experimental deflection on each point. The calculation of theoretical deflection is reviewed in the Appendix F. The values of experimental and theoretical deflection of aircraft composite spoiler hinges are tabulated in Table 4.4 below.

Table 4.4: Experimental and Theoretical deflection of Aircraft composite spoiler hinges

Point	Load (kN)	Experimental compression Deflection, $y_{experiment}$ (mm)	Theoretical calculation Deflection, $y_{theoretical}$ (mm)	Percentages error (%)
1	2	-0.3	-0.13	57
2	6	-1.05	-0.48	54
3	10	-1.68	-0.63	62

Based on Table 4.4, there are slightly different between experimental and theoretical deflection for all point. In addition, the percentages error for point 1, 2 and 3 which are 57 %, 54% and 62% respectively. Moreover, the structural analysis of deflection also investigates this problem by comparing the experimental and theoretical deflection with the simulation finite element method deflection. The illustration of aircraft composite spoiler hinge deflection is shown in Figure 4.11.

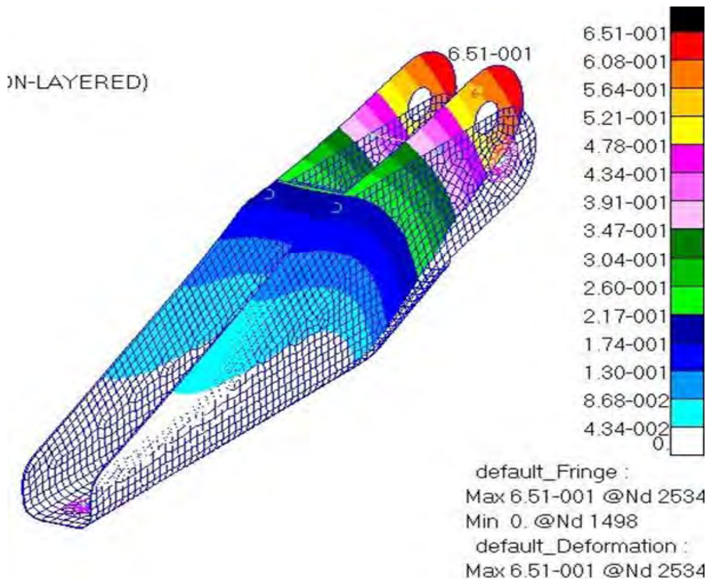

Figure 4.11: Hinge deformation at load of 10 kN (CTRM, 2017)

According to the Figure 4.11, the simulation finite element method analyzed the deflection by exerting a load of 10 kN to the hinge and located the fixed point on the holes of the bolt. The result is obtained through the maximum deflection occurred in the hinge. The maximum deflection of hinge occurred on the holes of the lug which similar to the experimental and theoretical deflection. The comparison deflection between experimental, theoretical and simulation are tabulated in Table 4.5.

Table 4.5: Deflection comparison between experimental, theoretical and simulation method at 10 kN

Load (kN)	Experimental compression Deflection, $y_{experiment}$ (mm)	Simulation of Finite Element Method Deflection, $y_{simulation}$ (mm)	Theoretical calculation Deflection, $y_{theoretical}$ (mm)	Percentages Error (%)
10	-1.68	-0.651	-0.63	61 - 63

According to Table 4.5, the value of theoretical and simulation deflection is showed almost similar but slightly different which compared to experimental deflection. The different value of experimental deflection compared to theoretical and simulation deflection as generally can be influenced by the low quality of manufacturing hinges or improper fabrication setup.

Moreover, the aircraft composite spoiler hinges or specimen of this testing is provided by the engineer of CTRM which pursuing a master course in UTeM. The improper manufacturing method is one of a major problem in quality performance in the laminated composite. The composite hinge is manufactured by Prepreg Autoclave fabrication method and manual-trimming without using any modern equipment and machine. The manufacturing process and work flow of fabrication are shown from Figure 4.12 until 4.14.

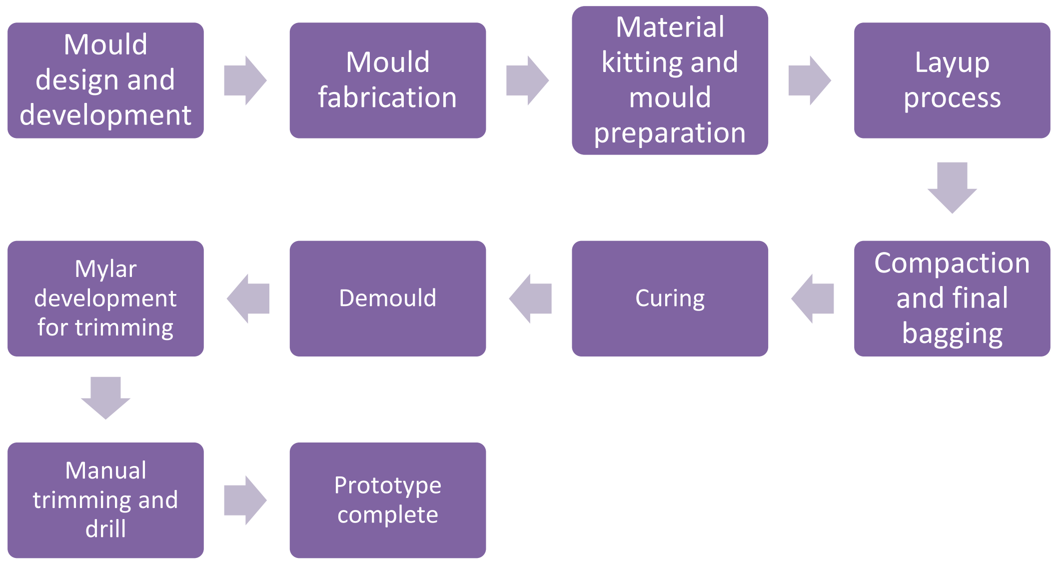

Figure 4.12: Process flow for prototype development process (Amirul CTRM, 207)

Figure 4.13: Laminated composite of Prepreg Autoclave Fabrication Method (Amirul CTRM, 2017)

Figure 4.14: Manual trimming and drilling (Amirul CTRM, 2017)

According to the Figure 4.12 until 4.14, the quality of aircraft composite spoiler hinge manufactured by using prepreg autoclave fabrication method is dependent on the skill of the operator. The fabrication process also is faced some problem due to the improper design of mould which contains void and vacancy between the mould and composite material. The void and vacancy between the mould and composite material will influence the non-uniform shape of the composite when the curing process applied temperature and pressure. However, the physical structural analysis has detected some defects on the composite hinges before testing. The defects are detected on the specimen such as wrinkle and non-uniform dimensional as shown in Figure 4.15 and 4.16 below.

Figure 4.15: Wrinkle

Figure 4.16: non-uniform shapes

Therefore, the defects experienced by the aircraft composite spoiler hinges indirectly influence the experimental result. Furthermore, the physical structural analysis also investigated the structural weak point of the aircraft composite spoiler hinges. The weak point is determined after the hinges failed. The location of hinge's weak point is located around the area of the holes of lug as shown in Figure 4.17 below.

Figure 4.17: Weak point of experimental testing

However, the experimental weak point location of hinges also will be compared to the weak point of hinges model through simulation of finite element method which provided by the engineer of CTRM. The stress distribution of hinges model can be described the possibility of weak point occurred and the Figure 4.18 below is showed stress distribution of hinges model.

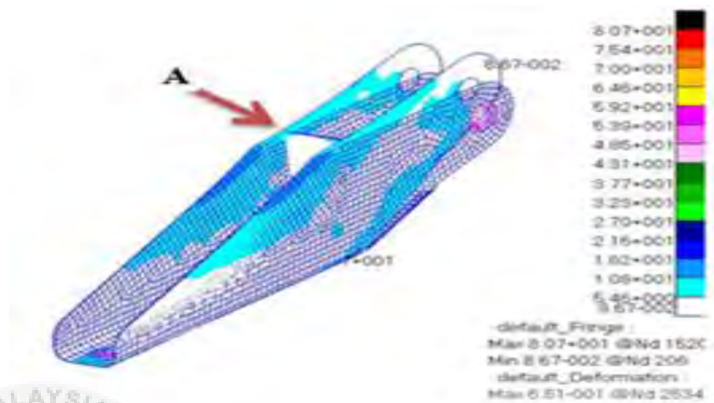

Figure 4.18: Stress distribution hinges model

According to the Figure 4.18, the highest stress distribution of hinges model is located on the holes of bolt and lug. But, the highest stress distribution occurred in holes of bolt and lug due to numerical error (W. C. Mun, 2014) and it also can be eliminated after applied tighten screw, bolt and nut during real application. Therefore, the blue colour area of point A and B on hinges model as shown in figure 4.15 will be another crucial weak point and interesting location to be investigated. Based on the failure criterion of brittle material as reviewed in chapter 2.3.3, the brittle material is weak when exposed to the tensile stress than compression stress because the compression stress has larger area region in Mohr's criterion diagram as shown in Figure 2.16. Therefore, the location A as shown in Figure 4.17 and 4.18 are relevant to be the first point fail or break due to highest bending moment and tensile stress at that location.

Lastly, the deflection and weak point of experimental testing have validated by simulation finite element method. The weak point location and first fail location of experimental testing are supported by simulation analysis as relevant location. For deflection analysis, the result of experimental deflection is slightly different with theoretical and simulation deflection. This phenomenon may occur due to the improper fabrication process of specimen manufacturing where the defects can be detected before testing. Therefore, the manufacturing process of the specimen must be more competent and try to reduce the defect. Also, the optimization design of composite hinges must be conducted by focusing more at the weak or critical point.

CHAPTER 5

CONCLUSION AND RECOMMENDATION

5.1 Conclusion

As mentioned earlier in the introduction, this research was undertaken with the aim of developing custom jig for real condition testing in the laboratory as well as investigate structural of aircraft composite spoiler hinge by comparing and validating between experimental and simulation finite element method result. The testing was tried to taking the real condition of aircraft operation into consideration when conducting an experiment in the laboratory. The real condition testing was separated into two experiments with respect to the superposition method. The superposition method was applied to solve limitation problem of tester machine which cannot exert two loads at one time. Unfortunately, the second experiment which is testing for hinge moment was experienced slipping jig and the results were not applicable for interpretation of the structural analysis. Therefore, the structural analysis of composite hinges was still identified by conducting another compression testing. The result of compression testing in term of fail location and deflection of composite hinges were used to compare with the theoretical and simulation finite element method. Therefore, the location of the weak point and first point break were determined in location A as shown in Figure 4.14 and 4.15 due to highest bending moment and tensile stress. Moreover, the three-point deflection of linear curve compression testing result was compared to experimental and theoretical calculation where the percentages error between them shown 57%, 54% and 62% for point 1, 2 and 3 respectively. In addition, the experimental deflection of 10 kN compressive loads also was compared with the same load deflection of simulation finite element method and theoretical calculation deflection. The result was obtained deflection different between them in the range 61% and 63%. The different values of deflection were caused by low-quality manufacturing and improper fabrication method of the composite hinge. This is because the several defects were detected before the testing is conducted such as wrinkle, non-uniform thickness and non-uniform shape. In nutshell, the defects experienced by composite hinge indirectly influenced the result between experimental testing and simulation of finite element method. The improvement of aircraft composite spoiler hinges is required in term of the manufacturing process in order to achieve better quality and performance.

5.2 Recommendation

The experimental testing carried out in this research is only investigated on the aircraft composite spoiler hinges structural analysis in term of critical point and deflection based on compression testing result. Therefore, the result of this testing does not cover for the real condition of aircraft operation as earlier planning of the research due to slipping occurred between the custom jig and composite hinge. Besides that, the experimental testing is conducted in the laboratory also required considerable cost and lot of time spending. A detailed analysis of stress distribution through experimental testing cannot be analyzed due to lack of equipment such as there is no appropriate strain gauge for composite hinges in the laboratory. In other hands, the imperfection of aircraft composite spoiler hinges such as wrinkle and non-uniform shape are detected before testing. These defects may occur due to improper consideration of mould design where the void between the mould and composite material influence the quality of composite hinges.

Thus, it is a recommendation for further research to investigate the maximum stress experienced by aircraft composite spoiler hinges due to the real condition of aircraft operation. The real condition testing which mimics the operation of aircraft cannot be conducted due to slipping of the custom jig. Therefore, the custom jig was slipped in this research must be modified to be permanently connected with the composite hinge. Furthermore, the experimental testing also should be used the strain gauge in order to collect more accurate result, especially for stress distribution. The origin defect also should be minimizing by redesign the mould in order to eliminate vacancy space between the mould and composite material. The trimming process of composite hinges should be using CNC machine in order to develop accurate dimension of the product.

REFERENCES

A. Baker, D. K. (2004). *Composite Materials for Aircraft Structures.* United States of America: American Institute of Aeronautics and Astronautic Inc.

ASM. (2004). *Introduction to Tensile Testing; Tensile Testing, Second Edition.* ASM International.

B. Wanga, P. L. (2016). Symplectic superposition method for new analytic buckling solutions of. *International Journal of Mechanical Sciences*, 432–441.

Barbero, E. J. (2011). *Introduction to composite materials design: second edition.* United States of America: Taylor and Francis Group.

Broutman, S. K. (1993). *Applied Stress Analysis of Plastics: A Mechanical Engineering Approach.* Springer Science & Business Media.

Cairns, D. S. (2009). Composite Materials for Aircraft Structure. *Department of Mechanical and Industrial Engineering of Montana State University* (pp. 5-11). Montana State: Bozeman, Mountain & Minds.

Chawla, K. K. (2012). *Composite Materials: Science and Engineering.* New York: Springer Science & Business Media.

Dawson, D. (2006, January 7). *High performance composites*. Retrieved from Function and operation of aircraft spoilers: http://www.compositesworld.com/articles/function-and-operation-of-aircraft-spoilers

Dewolf, F. P. (2011). *Mechanics of Material Fifth Edition in SI Units.* Singapore: McGraw Hill.

Fantuzzi, F. T. (2014). *Mechanics of laminated Composite doubly-curvel shell structures.* Societa Editrice Esculapio.

Fenner, R. T. (2001). *Mechanics of Solids.* New York: CRC Press.

Gay, D. (2014). *Composite Materials: Design and Applications, Third Edition.* United States of America: CRC Press, Taylor & Francis group.

Grandt. (2004). *Fundamentals of Structural Integrity: Damage Tolerant Design and Nondestructive Evaluation.* New Jersey: John Wiley & Sons, Inc.

Groh, R. (2015). *Aerospace Engineering*. Retrieved from Introduction to Composite Materials: http://aerospaceengineeringblog.com/composite-materials/

Gurdal Z., H. R. (1999). *Design and Optimization of Laminated Composite Materials.* New York: John Wiley & Sons.

H. Altenbach, J. W. (2013). *Mechanics of Composite Structural Elements.* Berlin: Springer.

Hoa, S. V. (2009). *Principles of the Manufacturing of Composite Materials.* United States of America: DEStech Publications, Inc.

Holmes, R. H. (2011). *History of Recent Science & Technology*. Retrieved from General overviews of materials research history: http://authors.library.caltech.edu/5456/1/hrst.mit.edu/hrs/materials/public/general.htm

Hopkins, S. N. (2004). *Strength of Material: A Unified Theory.* United States of Amireca: Elsevier Publication.

Houston, S. (2016, October 13). *The Balance*. Retrieved from Advantages and Disadvantages of Composite Materials on Airplanes: https://www.thebalance.com/composite-materials-aircraft-structure-282777

Hull, T. W. (1996). *An Introduction to Composite Materials.* New York: Press Syndicate of the University of Cambridge.

Jones, R. M. (1998). *Mechanics Of Composite Materials.* Virginia: CRC Press.

Joyce, J. (2008). *Element*. Retrieved from Mechanical Testing: https://www.element.com/materials-testing-services/mechanical-testing-services#

Kassapoglou, C. (2011). *Design and Analysis of Composite Structures: With Applications to Aerospace Structures.* United States of America: John Wiley & Sons.

Lewis, S. J. (1994). The use of carbon fibre composites on military aircraft. *Composite Structures*, 95-103.

M. Abedi, R. A. (2015). A new solution method for free vibration analysis of rectangular laminated composite plates with general stacking sequences and edge restraints. *Computers & Structures*, 144–156.

Mallick, P. K. (1997). *Composites Engineering Handbook.* New York City: Marcel Dekker, Inc.

Mukhopadhyay, M. (2005). *Mechanics of Composite Materials and Structures.* India: Universities Press (India) Private Limited.

Nasa. (2010). *National Aeronautics and space administration*. Retrieved from Spoilers: https://www.grc.nasa.gov/www/k-12/airplane/spoil.html

Paavola, Q. L. (2015). Lightweight design of composite laminated structures with frequency. *Composite Structures*, 356–360.

Pandey, P. C. (2004). Retrieved from Composite Materials.: http://nptel.iitk.ac.in/ courses/Webcourse-contents/IIScBANG/Composite%20Materials/Learning%20material %20-%20composite%20material.pdf.

Reddy, J. N. (2004). *Mechanics of Laminated Composite Plates and Shells: Theory and Analysis, Second Edition.* United States of America: CRC Press Inc.

Rofles, M. B. (2017). Revealing complex aspects of compressive failure of polymer composites – Part II: Failure interactions in multidirectional laminates and validatio. *Composite Structures*, 116-128.

Sadraey, M. (2014). *Spoiler Design.* Nashua, New Hampshire: Daniel Webster College.

Sierakowski, J. R. (2012). *The behavior of structures composed of composite materials.* United States of America: Kluwer Academic Publisher.

Steif, P. S. (1999). A Model of Kinking in Fiber Composite- Fiber Breakage via Micro-Buckling. *Solid Structure and Composites*, 549-561.

V.A. Komarov, E. K. (2015). Aircraft composite spoiler fitting design using the variable density model. *International Conference on Communication, Management and Information Technology*, 99 – 106.

W. C. Mun, A. R. (2014). Design and Analysis of an Aircraft Composite Hinge Bracket using. *Applied Mechanics and Materials Vol. 629*, 158-163.

W. Roeseler, B. S. (2015). COMPOSITE STRUCTURES: THE FIRST 100 YEARS. *16TH INTERNATIONAL CONFERENCE ON COMPOSITE MATERIALS.* Kyoto, Japan: The Boeing Company.

W. Xiao, L. l. (2016). Accurate modal superposition method for harmonic frequency response sensitivity of non-classically damped systems. *Mechanical Systems and Signal Processing*, 204–217.

ZiaeRada, A. K. (2014). Experimental and analytical study on fiber-kinking failure mode of laminated composites. *Composites Part B: Engineering*, 84-93.

APPENDIX A

Airbus A320 Spoiler General Arrangement Drawing (Courtesy of Spirit Aerosystem)

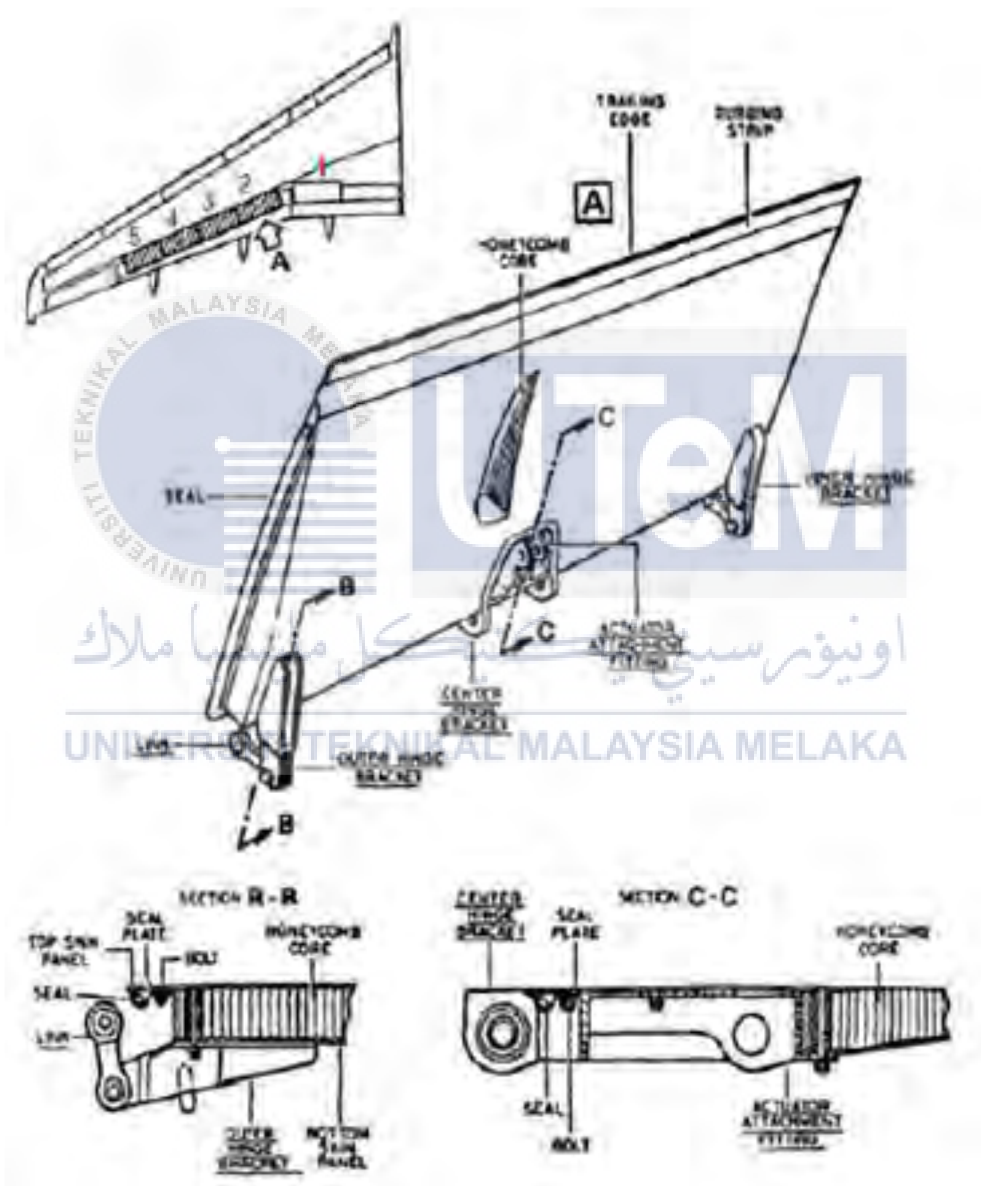

APPENDIX B

Airbus A320 Original Hinge Bracket Drawing (Courtesy of Spirit Aerosystem)

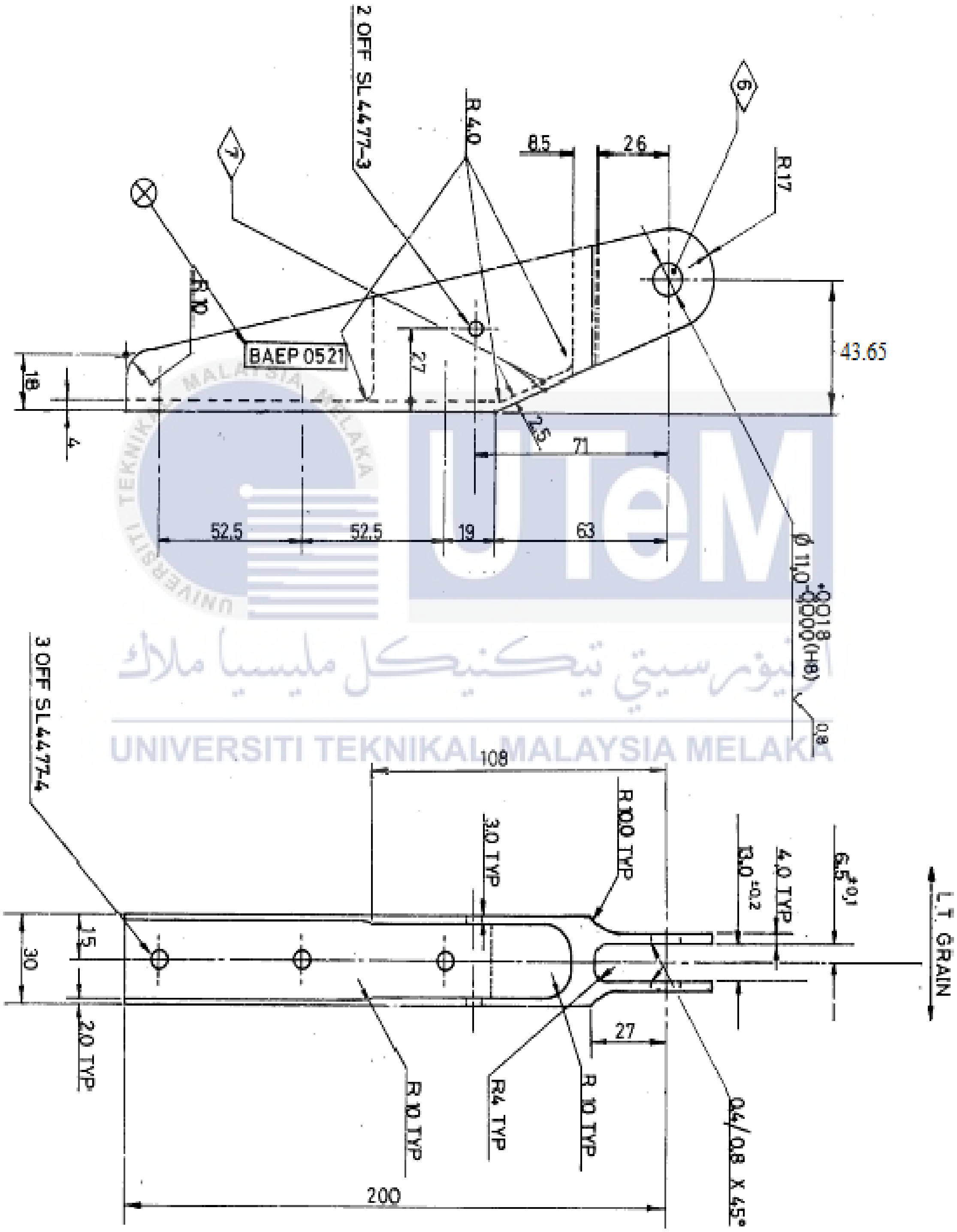

APPENDIX C

Airbus A320 Load Cases

Airbus A320 Hinge Loads (Courtesy of Spirit Aerosystem)

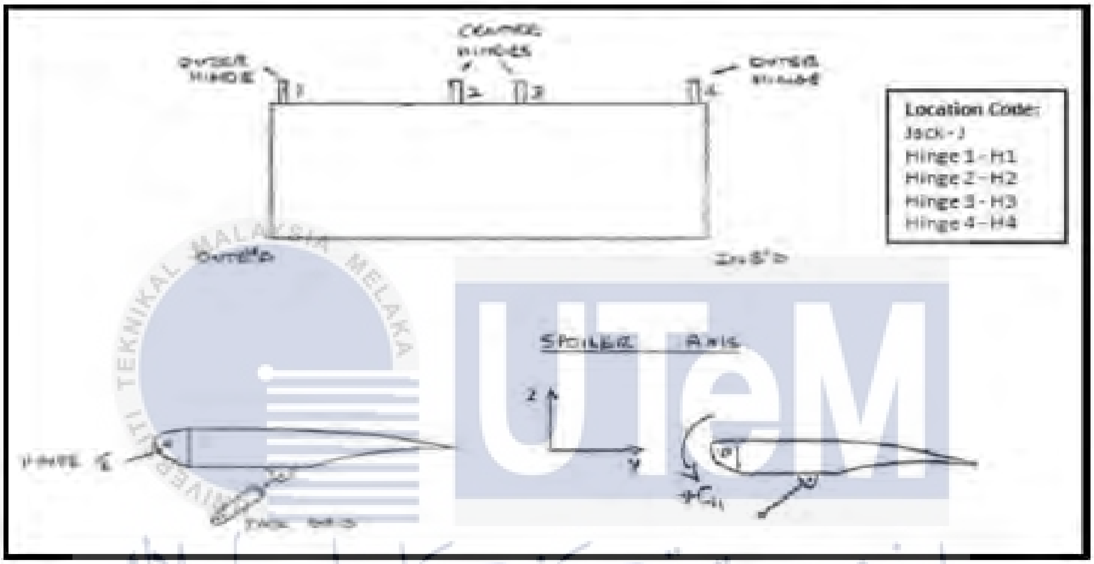

Jack and Hinges Location/Axis

Summary of Hinge 4 Loads with Wing Deflections.

Case		Loads (Factorized)			
		Y (N)	Z (N)	Resultant (N)	Moment (Nm)
C, 20°	No wing bending	-537	3685	3724	-7310
	+ve wing bending	-671	4899	4648	
	-ve wing bending	-423	2904	2935	
B, 0°	No wing bending	407	-2793	2822	6805
	+ve wing bending	274	-1878	1898	
	-ve wing bending	521	-3573	3611	

Summary of Hinge 4 Loads without Wing Deflections.

Case	Loads (Unfactored)			
	Y (N)	Z (N)	Resultant (N)	Moment (Nm)
A, 0°	-195	-1335	1349	-5040
B, 0°	244	-1676	1693	4142
C, 5°	-357	2447	2473	-4900
C, 10°	-346	2374	2399	-4750
C, 15°	-336	2302	2327	-4600
C, 20°	-324	2220	2244	-4430
C, 25°	-311	2134	2157	-4250
C, 30°	-270	2037	2055	-4050
C, 35°	-283	1940	1961	-3850
C, 40°	-267	1832	1851	-3625
C, 45°	-249	1710	1728	-3375
C, 50°	-230	1576	1593	-3100

Note:

1) All loads are in spoiler axis as defined in figure above.

2) Ult/Lit Factor = 1.1 x 1.5 (on airload).

APPENDIX D

Dimensional of Custom Jig Design for Experimental Testing

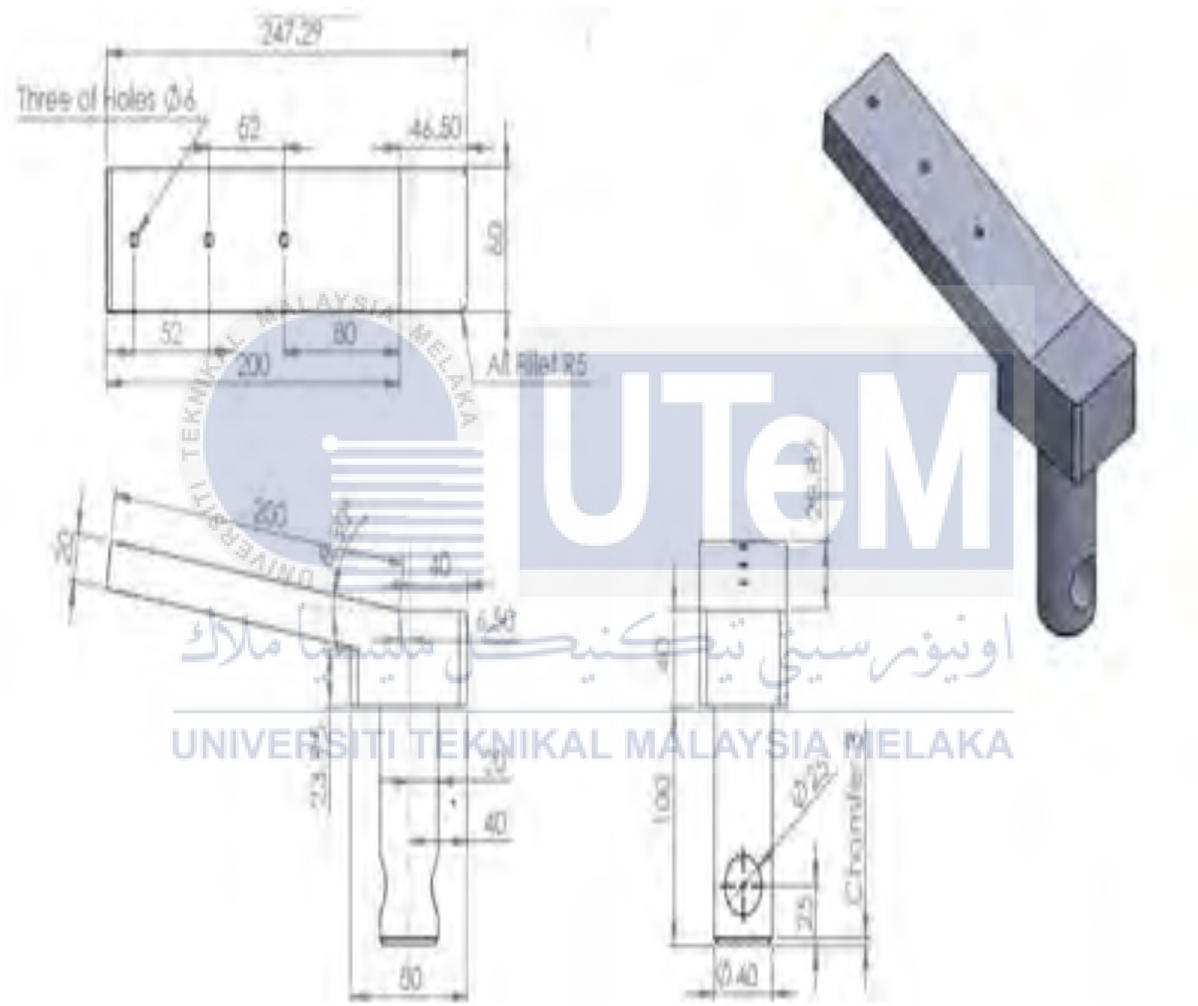

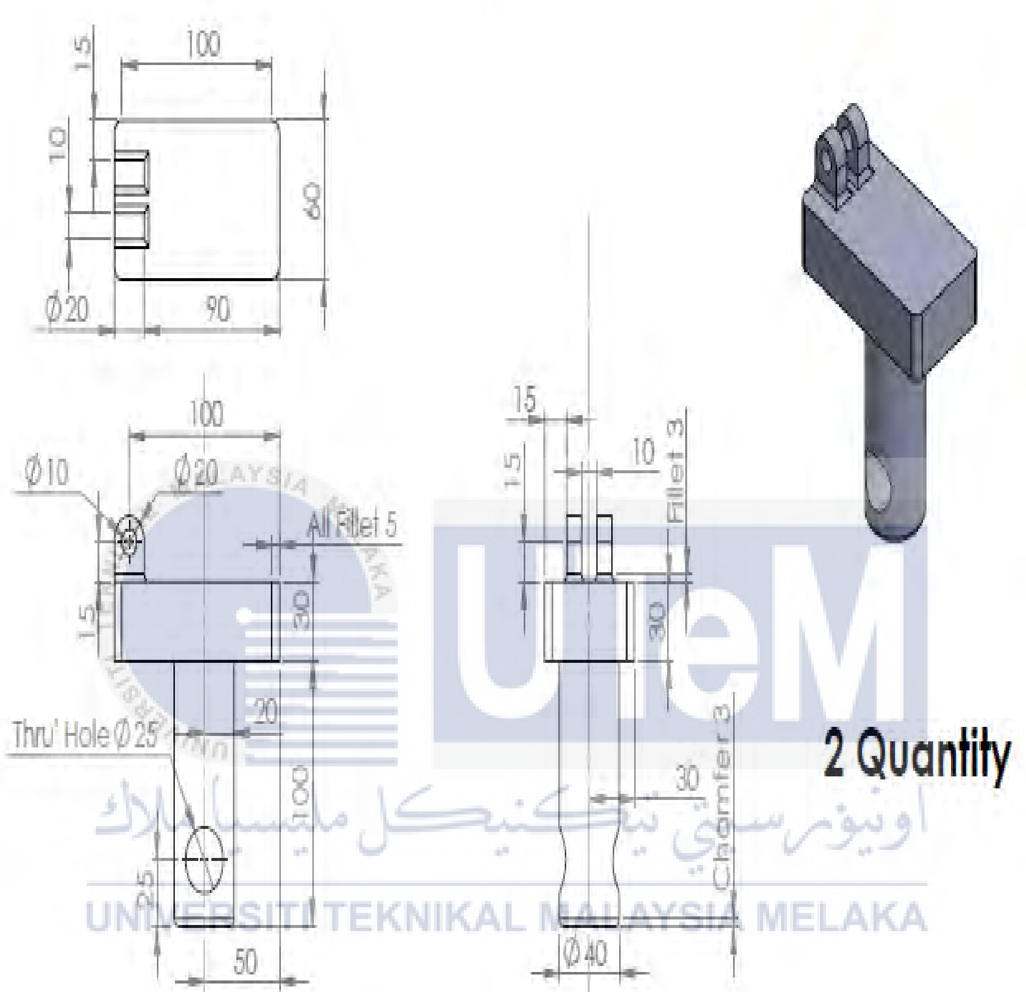

100
15
10
60
Ø20
90
100
Ø10
Ø20
All Fillet 5
15
30
20
Thru' Hole Ø25
100
25
50
15
15
10
Fillet 3
30
Chamfer 3
30
Ø40
2 Quantity


40
20
10
50
Ø10
R15
100
Ø30
205
Ø11
Ø15
Ø10

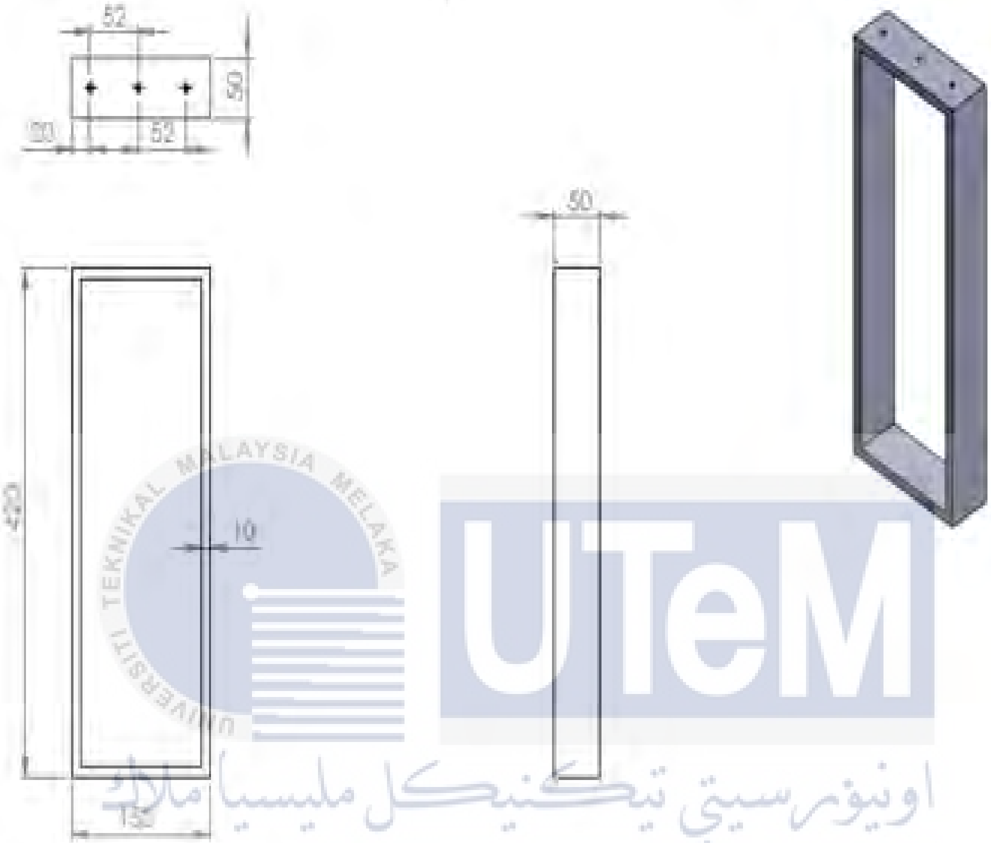
52
50
20
52
50
420
10
150

APPENDIX E

FEA Result of Metallic and Composite Spoiler Hinges

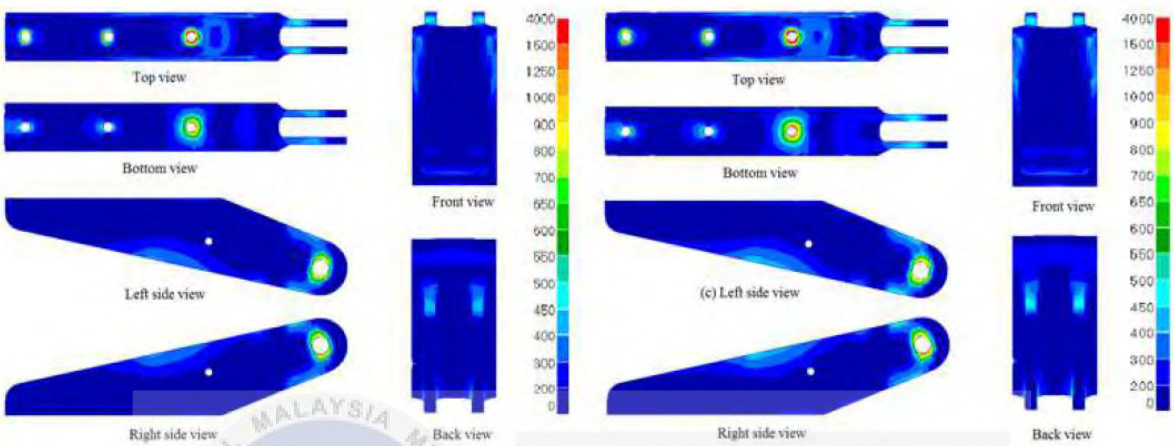

(a) (b)

Stress Distribution of Original Hinges

Comparison of Stresses at the Bolt and Lug Holes of the original Hinge Bracket

Case		Von Mises Stresses			
		Bolt		Lug	
		Nastran	Abaqus	Nastran	Abaqus
Spoiler close	No wing bending	1888.67	1890.59	842.083	841.171
	+ve wing bending	1751.50	1752.65	839.882	838.970
	-ve wing bending	1997.80	2000.37	843.971	843.058
Spoiler open	No wing bending	2117.22	2120.62	908.117	907.134
	+ve wing bending	2286.98	2272.59	910.938	905.301
	-ve wing bending	2008.14	2010.88	906.231	905.248

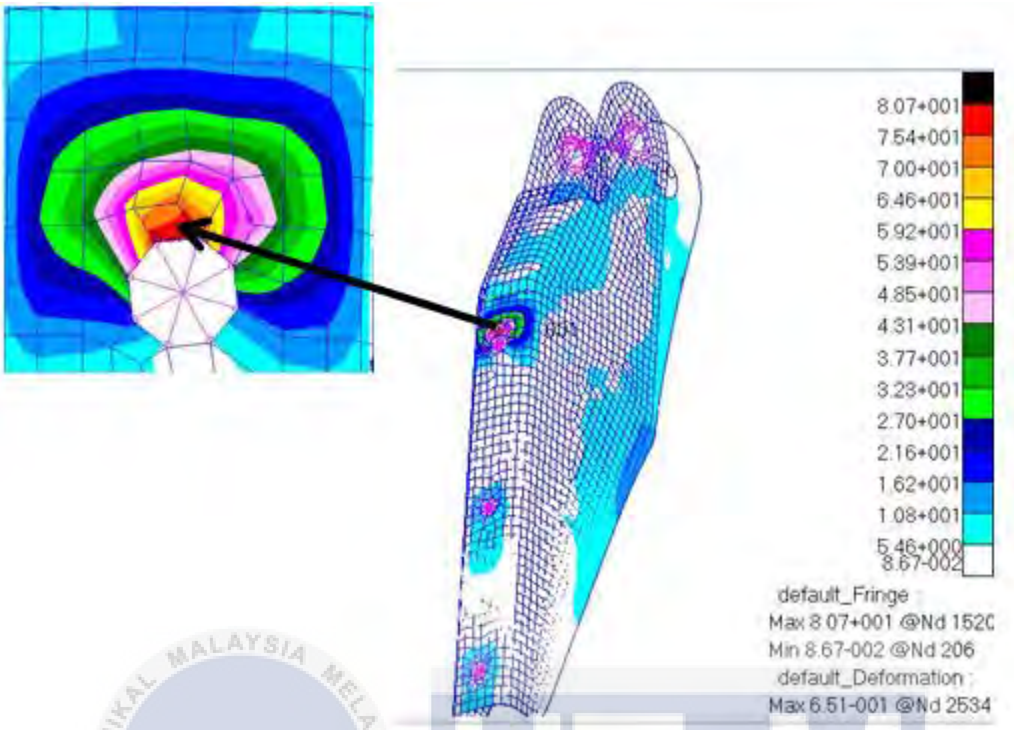

Maximum stress occurred at mounting hole

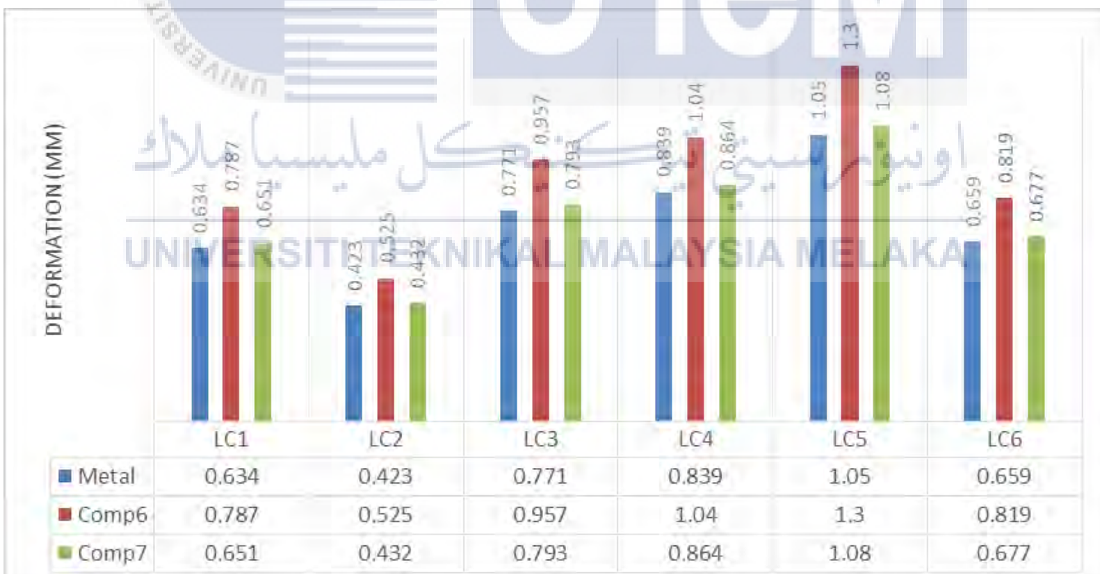

Hinge deformation baseline result for three different material and properties arrangement chart

APPENDIX F

Calculation of Theoretical Deflection using Compression Testing Result

1. Determination moment of inertia of composite hinges

   By considering hinges as uniform cross section and only focus on a critical area which is at the holes of the lug.

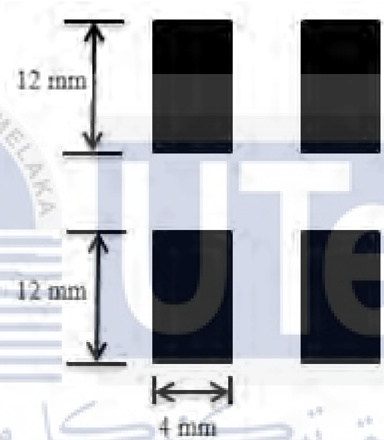

$I = \frac{bh^3}{12} \times 12$ mm

$I = \frac{(0.004)(0.012)^3}{12} \times 4$

$I = 2.304 \times 10^{-9}$ m^4

2. Determination deflection of theoretical calculation of composite hinges

   Deflection of theoretical calculation of composite is determined by using equation (2.25). By referring Figure 4.10, the load, P of three points is used to determine theoretical deflection. The distance, L is the distance between load and maximum bending of hinges which it measured by 0.031 m and Equivalent modulus of composite hinges is provided from a simulation which given by 68 GPa. The load at each point is tabulated at the table below:

Point	Load (kN)
1	2
2	6
3	10

Point 1:

$$y = -\frac{PL^3}{6EI}$$

$$y = -\frac{(2000)(0.031)^3}{6(68\times10^9)(2.304\times10^{-9})}$$

$y = -0.13$ mm

Point 2:

$$y = -\frac{PL^3}{6EI}$$

$$y = -\frac{(6000)(0.031)^3}{6(68\times10^9)(2.304\times10^{-9})}$$

$y = -\ 0.38$ mm

Point 3:

$$y = -\frac{PL^3}{6EI}$$

$$y = -\frac{(10000)(0.031)^3}{6(68\times10^9)(2.304\times10^{-9})}$$

$y = -\ 0.634$ mm